ANKARA YILDIRIM BEYAZIT UNIVERSITY

GRADUATE SCHOOL OF NATURAL AND APPLIED SCIENCES

TITANIUM DIBORIDE (TiB_2) REINFORCED SILVER (Ag) BASED NANOCOMPOSITE COATINGS BY ELECTRODEPOSITION METHOD

M.Sc. Thesis by

Dila COŞMUŞ

Department of Materials Engineering

December, 2021

ANKARA

TITANIUM DIBORIDE (TiB_2) REINFORCED SILVER (Ag) BASED NANOCOMPOSITE COATINGS BY ELECTRODEPOSITION METHOD

A Thesis Submitted to

the Graduate School of Natural and Applied Sciences of

Ankara Yıldırım Beyazıt University

In Partial Fulfillment of the Requirements for the Degree of Master of Science in Materials Engineering, Department of Metallurgical and Material Engineering

by

Dila COŞMUŞ

December, 2021

ANKARA

M.Sc. THESIS EXAMINATION RESULT FORM

We have read the thesis entitled "**TITANIUM DIBORIDE (TiB_2) REINFORCED SILVER (Ag) BASED NANOCOMPOSITE COATINGS by ELECTRODEPOSITION METHOD**" completed by **DİLA COŞMUŞ** under supervision of **Assoc. Prof. Dr. RAMAZAN KARSLIOĞLU** and we certify that in our opinion it is fully adequate, in scope and in quality, as a thesis for the degree of Master of Science.

Assoc. Prof. Dr. Ramazan KARSLIOĞLU

Supervisor

Prof. Dr. Aytunç ATEŞ

Jury Member

Assist. Prof. Bilge IMER

Jury Member

Prof. Dr. Sadettin ORHAN

Director

Graduate School of Natural and Applied Sciences

ETHICAL DECLARATION

I hereby declare that, in this thesis which has been prepared in accordance with the Thesis Writing Manual of Graduate School of Natural and Applied Sciences,

- All data, information and documents are obtained in the framework of academic and ethical rules,
- All information, documents and assessments are presented in accordance with scientific ethics and morals,
- All the materials that have been utilized are fully cited and referenced,
- No change has been made on the utilized materials,
- All the works presented are original,

and in any contrary case of above statements, I accept to renounce all my legal rights.

Date: **Signature:**

Name & Surname: Dila COŞMUŞ

ACKNOWLEDGEMENTS

First and foremost, I would like to express my deep and sincere gratitude to my advisor Assoc. Prof. Dr. Ramazan KARSLIOĞLU for his limitless support, encourage, patience and guidance helped me to complete this thesis.

I would also like to thank National Boron Research Institute for enabling me to carry out this study by supporting our project named “The effects of addition of nano B_2O_3, B_4C c-BN, h-BN, TiB_2 and ZrB_2 on the contact performance of Ag-based electrical contact materials” (project number: 2019-30-07-25-001).

Finally, I would like to thank my family for their love, trust and support which helped me to complete this study.

2021, December **Dila COŞMUŞ**

TITANIUM DIBORIDE (TiB_2) REINFORCED SILVER (Ag) BASED NANOCOMPOSITE COATINGS BY ELECTRODEPOSITION METHOD

ABSTRACT

Silver is one of the most used materials in electrical industry due to its excellent electrical and thermal conductivity properties and it is frequently used as electrical contact material. However, silver's low mechanical strength has prompted researchers to produce different electrical contact materials. Many studies have been carried out by reinforcing a different material into silver (adding a second phase). In this study, titanium diboride reinforced silver based nanocomposite coatings are produced in order to obtain a new generation contact material with longer service life, economical, safer, environmentally friendly and most importantly, good contact performance. Titanium diboride is a promising material for electrical contacts with its excellent features such as high hardness, high melting temperature, low density, low electrical resistivity, good thermal conductivity.

In this study, unreinforced silver and titanium diboride reinforced silver based nanocomposite coatings produced by electrodeposition technique with using direct current, pulse current and pulse reverse current methods on copper substrates. Firstly, nanocomposite coatings were produced with the addition of 0.5, 1.0, 2.0 and 4.0 gram/Liter titanium diboride into electrolyte and effects of reinforcement with different amounts in silver matrix were analyzed. 1.0 gram/Liter titanium diboride reinforced silver based nanocomposite coatings were also produced with using direct current, pulse current and pulse current methods. All coatings were analyzed by Scanning Electron Microscope, Energy Dispersive Spectroscopy, X-ray Diffraction Analysis, Vickers Microhardness Test, Electrical Resistivity Measurements, Cross-Sectional Analysis, Electrical Contact Performance Test and Corrosion Resistance Tests.

Keywords: Silver, Titanium Diboride, Electrodeposition, Electrical Contact Materials.

ELEKTRODEPOZİSYON YÖNTEMİ İLE TİTANYUM DİBORÜR (TiB_2) TAKVİYELİ GÜMÜŞ (Ag) ESASLI NANOKOMPOZİT KAPLAMALARI

ÖZ

Gümüş, mükemmel elektriksel ve ısıl iletkenlik özelliklerinden dolayı elektrik endüstrisinde en çok kullanılan malzemelerden biridir ve sıklıkla elektrik kontak malzemesi olarak kullanılmıştır. Bununla birlikte, gümüşün düşük mekanik mukavemeti, araştırmacıları farklı elektrik kontak malzemeleri üretmeye sevk etmiştir. Farklı bir malzemeyi gümüşe takviye ederek (ikinci bir faz ekleyerek) birçok çalışma yapılmıştır. Bu çalışmada titanyum diborür takviyeli gümüş esaslı nanokompozit kaplamaları, daha uzun servis ömürlü, ekonomik, daha güvenli, çevre dostu ve en önemlisi iyi kontak performanslı yeni nesil kontak malzemesi elde etmek için üretilmiştir. Titanyum diborür, yüksek sertlik, yüksek ergime sıcaklığı, düşük yoğunluk, düşük elektriksel direnci, iyi termal iletkenlik gibi mükemmel özellikleriyle elektrik kontakları için gelecek vaat eden bir malzemedir.

Bu çalışmada, takviyesiz gümüş ve titanyum diborür takviyeli gümüş esaslı nanokompozit kaplamaları bakır yüzeyler üzerinde doğru akım, puls akımı ve puls ters akımı yöntemleri kullanılarak elektrodepozisyon tekniği ile üretilmiştir. İlk olarak, nanokompozit kaplamaları elektrolite 0,5, 1,0, 2,0 ve 4,0 gram/litre titanyum diborür ilave edilerek üretilmiş, gümüş matrisinde farklı miktarlarda takviyenin etkileri analiz edilmiştir. 1,0 gram/litre titanyum diborür takviyeli gümüş esaslı nanokompozit kaplamaları ayrıca doğru akım, darbe akımı ve darbe ters akımı yöntemleri kullanılarak üretilmiştir. Tüm kaplamalar Taramalı Elektron Mikroskobu, Enerji Dağılımlı Spektroskopi, X-ışını Kırınım Analizi, Vickers Mikrosertlik Testi, Elektriksel Direnç Ölçümleri, Kesitsel Analiz, Elektrik Kontak Performansı Testi ve Korozyon Direnci Testleri ile analiz edilmiştir.

Anahtar Kelimeler: Gümüş, Titanyum Diborür, Elektrodepozisyon, Elektrik Kontak Malzemeler

CONTENTS

NOMENCLATURE

Abbreviations

µm	Micrometer
Å	Angstrom
°C	Celsius Degree
A	Ampere
Ag	Silver
$AgNO_3$	Silver Nitrate
Al	Aluminum
Al_2O_3	Aluminum Oxide
Au	Gold
B	Boron
C	Carbon
Cd	Cadmium
CdO	Cadmium Oxide
CTAP	Hexadecyltrimethylammonium Bromide
Cu	Copper
g	Gram
Gr	Graphene
I	Current
KCN	Potassium Cyanide
l	Liter
Mg	Magnesium
mA	Milliampere
NaCl	Sodium Chloride
Ni	Nickel
nm	Nanometer
PANI	Polyaniline
PET	Polyethylene Terephthalate
Pd	Palladium
PPS	Polyphenylene Sulfide
PS	Polystyrene
Pt	Platinum

PVA	Polyvinyl Alcohol
R	Resistivity
Rpm	Round per minute
SDS	Dodecyl Sulfate Sodium Salt
Si	Silicon
SiC	Silicon Carbide
Si_3N_4	Silicon Nitride
Sn	Tin
Ti	Titanium
TiB_2	Titanium Diboride
V	Voltage
W	Tungsten
WC	Tungsten Carbide
ZnO	Zinc Oxide
Zr	Zirconium
ZrO_2	Zirconium Dioxide

Acronyms

AC	Alternative Current
CMC	Ceramic Matrix Composites
CMNC	Ceramic Matrix Nanocomposites
CNTs	Carbon Nanotubes
CVD	Chemical Vapor Deposition
DC	Direct Current
EDS	Energy Dispersive Spectrometer
FCC	Face-Centered Cubic
HV	Hardness Vickers
JCPDS	Joint committee on powder diffraction standards
KW	Kilowatt
MMC	Metal Matrix Composites
MMNC	Metal Matrix Nanocomposites
MWCNT	Multy-walled carbon Nanotubes
PC	Pulse Current

pH	Power of Hydrogen
PMC	Polymer Matrix Composites
PMNC	Polymer Matrix Nanocomposites
PRC	Pulse Reverse Current
PVD	Physical Vapor Deposition
SEM	Scanning Electron Microscopy
TEC	Thermal Expansion Coefficient
Ton	Pulse Current on-time
Toff	Pulse Current off-time
XRD	X-ray Diffractometer

LIST OF TABLES

LIST OF FIGURES

CHAPTER 1

INTRODUCTION

Electrical contact is an important component of electrical systems, and it serves completing or interrupting the electrical circuit. Due to their important role in switching devices, electrical contacts must have good physical and electrical properties for working in an efficient way. Electrical contacts must have properties such as high welding resistance, good arc erosion resistance properties as well as high electrical conductivity and low contact resistance properties in order to have a long service life [1-3]. Since the electrical contacts have an important role for carrying current or breaking the circuit, it is important to develop new promising electrical contact materials. After all, the failure of the contacts caused many accidents such as crash of the telephone system or even crash of an airplane in the past [4, 5].

The fire accidents due to electrical contact is the first or second reason in the countries such as U.S.A., England, Japan and even Istanbul city in Turkey. In Istanbul, between 110-120 fire accidents exist every day (according to data from 2017). Therefore, more than 25 fire accidents were occurred due to electrical contacts every day in Istanbul in 2017. When these numbers are compared with the data from 1985-1990, it can be clearly seen that there is a noticeable change in the rates of fire originating from electrical contacts. It can be stated that increase in technological developments and therefore increased electric source is the reason of that situation. The developments took place, but the number of electrical machines or instruments (e.g. in houses, schools, hospitals etc.) increased significantly over the years. And another reason for fire accidents originated from contacts can be not replacing the old electrical facilities [6].

Another reason to develop new contact materials is the harmful material usage in contacts. Cadmium Oxide (CdO) has been used since 1950s due to its unique properties such as good arc erosion resistance, low contact resistance and low welding resistance properties etc. However, in addition to these features, the production of contact materials by using CdO has been reduced or completely eliminated in many

countries due to the fact that it is not an environmental friendly material [7,8]. Therefore, it is necessary to develop new promising contact material that is both environmental friendly and has good electrical properties for electrical contacts to obtain better contact performance.

One of the most frequently used metals among electrical contact materials up today is the Silver (Ag). Ag has the distinction of being the metal with the highest electrical and thermal conductivity properties among all metals [9]. Also, it has been stated in the literature that adding a second phase to the electrical contact material can prevent the deterioration that occurs due to contact performance on the contact surfaces [10]. In addition, it is known that the Ag-CdO is frequently used in electrical contacts, even called "Universal Contact" in literature [7]. Accordingly, in this study, it was aimed to improve the performance of electrical contacts by adding a second phase into the Ag base.

Within the scope of this study, using TiB_2 as a second phase material instead of an environmentally harmful material such as CdO is aimed. TiB_2 is a ceramic material with hexagonal structure. It promises to be a good electrical contact material with its properties such as high hardness, low density, and low electrical resistivity properties etc. It is also known that when TiB_2 is used as a reinforcement material with metals, stiffness and hardness of these materials increased [11,12]. Thanks to its unique properties, TiB_2 will be used as a reinforcement material into the Ag matrix in this study.

Compared to other nanocomposite coating methods, electrodeposition is an easier and low-cost technique in terms of manufacturing. This technique provides uniform distribution of particles, continuous process and less waste materials than the others. It is stated in the literature that nanocomposite coatings can be produced by electrodeposition technique with using different methods such as Pulse Current and Pulse Reverse Current methods. By using these methods, controlling structure and properties of coatings become possible [13].

Thus, the aim of this study is developing new electrical contact material by producing Ag-TiB_2 nanocomposite coatings with different electrodeposition methods those are

DC, PC and PRC methods. In the scope of this study, the effects of TiB_2 reinforcement into Ag matrix, different amount of reinforcement and applied different current methods were investigated. The preference for the electrodeposition method for production allowed lower cost, usable at low temperature and easy to use. The unreinforced Ag and Ag-TiB_2 nanocomposite coatings were deposited on copper backings which are contact buttons and copper cylinders. The coatings were analyzed by Scanning Electron Microscope (SEM), Energy Dispersive Spectroscopy (EDS), X-ray Diffraction Analysis (XRD), Vickers Microhardness Test, Electrical Resistivity Measurements, Cross-Sectional Analysis and Corrosion Resistance Tests. Also, electrical contact performance tests were performed to get information about contact effects such as melting, arc erosion and welding which occurs during contact.

CHAPTER 2

LITERATURE REVIEW

2.1. Composite Materials

Composites have been a part of our lives for thousands of years. The first human-made composite may be mummification in Egypt. The oldest known mummy belongs to the year 3000 BC [14]. The knowledge and production methods of composites have been developed for over centuries. And now, production of composites takes place by selecting of right reinforcement and matrix materials with considering application area [15]. Composite materials consist of two or more materials which produces a material with excellent properties by comparison with the individual components. The resulting material (composite) of this combination occurs in macro level, however there is an important point that the composites are homogeneous materials in micro level. The excellent properties which can be obtained by producing composites can be stiffness, strength, electrical properties, and corrosion and wear resistance etc. The common reason to use composites is the low weight and high strength properties at the same time (Figure 2.1). Another common reason is that composites provide design flexibility. These advantages cause increasing attention on composite materials [16-19].

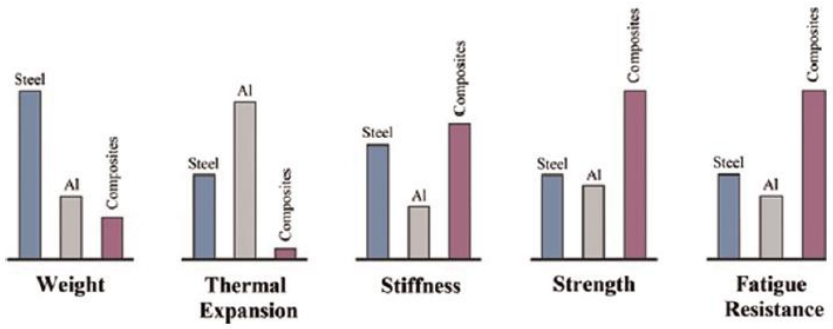

Figure 2.1 Comparison of physical and mechanical properties of composites, steel and aluminum [19].

2.1.1. Classification of Composite Materials

Composite materials consist of matrix (continues phase) material and reinforcement (discontinues phase) material embedded (Figure 2.2). When a force is applied, the matrix phase is responsible for transmitting and distributing this force to the reinforcement material. The matrix material is generally soft comparing with reinforcement material. And the interface between matrix and reinforcement materials transmits any force to the reinforcement material without any fracture or decomposition although it is generally fragile. The properties of composite materials depend on properties, contents, types and distributions of these components. Metals, polymers, ceramics and glass have been used mainly as reinforcement and matrix material. On the basis of used matrix, there are three classification of composites which are ceramic matrix composites, polymer matrix composites and metal matrix composites [17,19,20].

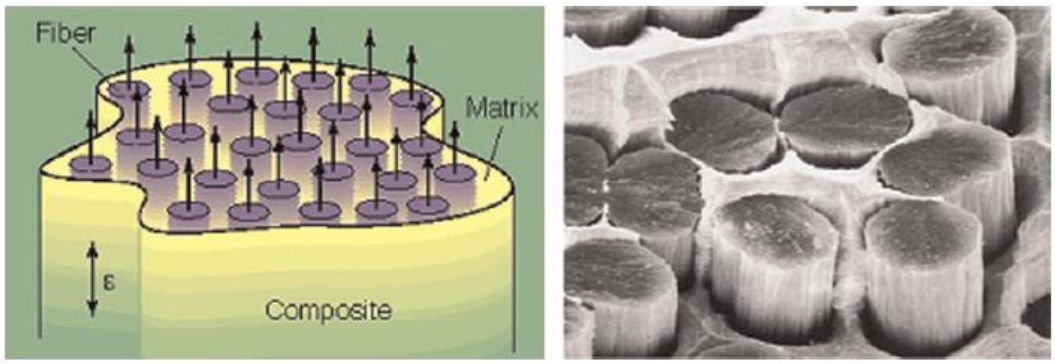

Figure 2.1 Schematic and real illustrations of composite structure [19].

2.1.1.1. Ceramic Matrix Composites

Ceramic matrix composites consist of ceramic matrix with fiber reinforcement. The reason to use fiber as reinforcement material is low ductility and toughness properties of ceramics [17]. Ceramics have excellent properties such as low density (low weight), high oxidation resistance (suitable for high temperature applications), wear resistance etc. However, their disadvantages such as being a brittle material and having low toughness makes harder their use in application areas such as defense industry and aviation applications. Therefore, intensive studies are carried out on the design,

production and characterization of CMCs in order to benefit from the advantageous properties of ceramics and at the same time to improve their toughness. In addition, when the scientific studies on CMCs are examined in recent years, it is seen that the studies have focused on microstructures that are less susceptible to cracking [21,22].

2.1.1.2. Polymer Matrix Composites

Polymer Matrix Composites consist of polymer matrix and reinforcement material which may be long or short fibers, particles or nanoparticles. PMCs are corrosion resistant, easy to produce and formable materials. Due to its easy handling techniques and simple fabrication methods, PMCs are low-cost materials. They are divided into two groups as thermoset and thermoplastic matrix composites. It should be stated that the thermosets are preferred more often than thermoplastics due to their higher strength and resistance to high temperature properties [17,22]. PMCs are frequently used in aircrafts, wind turbines, sports equipments etc. Owing to their high specific strength, high specific stiffness and low density properties, they have been used too often in aircrafts. For instance, while they were used 2-4 wt. % in military aircrafts such as the F14 and F15 in the 1970s, they are used approximately 70 wt. % in advanced military aircrafts today such as Eurofighter [23].

2.1.1.3. Metal Matrix Composites

Metal matrix composites consist of a metal matrix and reinforcement material which can be dispersed ceramic or metallic phases. Compared to alloys, MMCs ensures good resistance to aggressive environments, good erosion resistance, good fracture properties, higher strength and stiffness. It must be stated that the MMCs are used more than other composites. Compared to other composites, the superior properties of MMCs can be higher thermal and electrical conductivity, higher fire resistance, better radiation resistance, better process-ability etc.

MMCs are classified in different categories due to used matrix material. Some common MMCs are;

- Aluminum-based composites,
- Magnesium-based composites,

- Titanium-based composites,
- Copper-based composites,
- Silver-based composites [19,24].

2.1.2. Matrix Materials of Composites

Composites consist of two phases which are matrix and reinforcement. The reinforcement (second) phase may be harder or softer due to application. Reinforcement increases all of the mechanical characteristics of matrix while matrix provides required shape for the reinforcement. Although, the main goal of matrix is transferring loads to the reinforcement, it protects the reinforcement from abrasion and environmental attack at the same time. The metals and glass are used as matrix material, but these materials are very expensive. Polymers such as epoxy, more sophisticated thermosets and unsaturated styrene-hardened polyesters are commonly used as matrix material [25,26].

2.1.3. Reinforcement Materials of Composites

Reinforcement material is stronger than matrix material in composites. The properties which reinforcement materials should provide can be summarized as;

- Low density,
- High Young's Modulus,
- Good thermal stability,
- High compression and tensile strength,
- Economic efficiency etc. [19].

Reinforcements can provide all or one of these properties in composites. The shape, amount, size and distribution of reinforcement directly effects composite's performance. Fibers, particles or whiskers are used as reinforcement materials in composites. When reinforcement's shape is similar to needle-shaped single crystal, it is a whisker reinforcement. If it is similar in all dimensions, it is particle reinforcement. And if it is a filament (cut or continuous), it is a chopped-fiber or fiber reinforcement [27,28]. Fibers are widely used in composites due to their advantages. There are some

other important factors which affect their performance. Factors which influence the performance of composites due to used fibers can be summarized as fiber geometry, fiber orientation, fiber volume fraction, packing arrangement and fiber diameter.

Fiber geometry plays a very important role when it comes to the properties of composites. The fibers have the highest mechanical properties across the width. This situation causes composites to exhibit anisotropic properties. It is also known that higher aspect ratio of fibers (using longer fiber) provides higher efficiency of reinforcement. Fiber orientation causes the composites to gain direction-specific properties. Thanks to these features, the assembly of composites in suitable designs is provided. Another important factor, the fiber volume fraction, is the ratio of fiber to resin. Fiber volume fraction can be affected by orientation and packaging arrangement of fibers. These are the factors which affect the manufacturing process. As far as the fiber diameter is concerned, it can be said that smaller diameter fibers will provide more surface area, thus the surface area on which loads will be spread will also increase. Along with all these, the fiber and matrix interface is also of great importance. A good bond between fiber and matrix should be essential. Thus, the fiber architecture and fiber-matrix interface affect everything from the production of composites to the properties they will show in their use [15].

2.1.4. Application Area of Composites

Applications of composite materials are increasing significantly with respect to needs to improve performance. Composites are design flexible materials so on their properties can be changed according to applications. Being lightweight and strong properties make composites as winning materials in the industry. For instance, composites are used in automotive industry due to such these unique properties. In general, composites have been used in a wide range of applications such as mass transport, building, construction, electrical and electronics, medical, defense, textile (sports) etc.

Among composites, the MMCs have got attention in recent years due to their properties such as high strength, high stiffness, good wear resistance and better thermal conductivity. MMCs have been already used in aircraft structures, jet engines, rockets

space shuttle, automotive parts etc. Also, there are investments in the electric industry to get unique properties from composites and they used in conductive parts such as circuit breakers. In addition, MMCs have been used as electrical contact materials due their flexible and unique properties [29,30].

2.2. Electrical Contacts

Electrical contact is a switch that is responsible for passage of electrical current across the contact interface without any interruption. Since they are general for electrical machines, their functioning must be well to obtain better performance and safety of these machines [31,32]. In fact, electrical contact's failure caused an electrical problem in Large Hadron Collider (CERN) recently. An electrical problem took place because of overheating of an electrical splice. As a result, the relief valves were overpowered due to leaked out six tons of helium and 53 large superconducting magnets were damaged [33].

Electrical contacts are electrical circuit components located in electrical switches, relays and responsible for providing electricity transmission (depending on whether it is open or closed) without any interruption. It is obvious that there should be a good metal-metal contact between contact surfaces in order to ensure the transmission of electricity. In order to provide this good metal-to-metal contact, there are many studies in the literature for contact material studies. However, before the contact materials, the properties of the electrical contact surfaces, the characteristics of them which occur during electrical transmission on contact surfaces and what properties contact materials should have must be well understood.

2.2.1. Problems in Electrical Contacts

2.2.1.1. Electrical Contact Resistance

There are oxide or other surface contaminant films on electrical contact surfaces. And as it's known, there are asperities on all surfaces due to manufacturing processes. When the contact occurs (the closed state of the contacts) between pair of contacts, these asperities on the contact surfaces create the transmission paths called "a-spot" by piercing these films. In summary, the actual contact area is a smaller part of the

apparent contact area (Figure 2.3). And it must be stated that in a-spots, metal, which is formed by the piercing of the films, reacts with oxygen or other corrosive gases. This situation causes reducing metallic contact area and therefore reducing electrical contact.

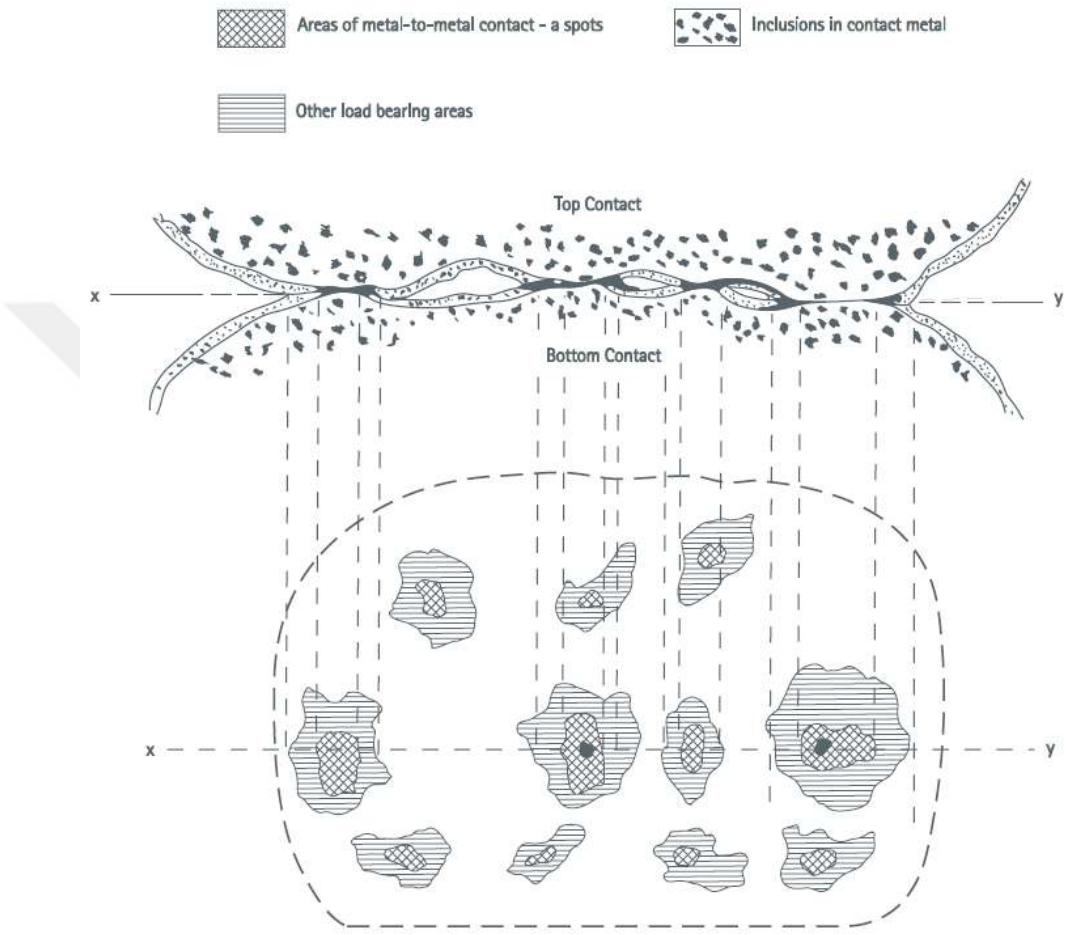

Figure 2.2 Illustration of true contact area on apparent contact area [34].

Contact force is an important factor in electrical contacts. If the force applied to the contacts is increased, the number and the area of a-spots increases. Therefore, it can be stated that the contact area is dependent on the applied force and is affected by the hardness of the softer contact material.

Current is constricted at contact interface while it passes through a-spots. The electrical contact resistance caused by this tight flow is called the constriction resistance (R_s). Pollution and oxides are among the factors that increase resistance. The constriction

resistance varies from metal to metal depending on the basic properties of metals such as hardness and electrical conductivity.

Total contact resistance of a joint is sum of the constriction resistance and the film resistance (caused by oxide, sulphide or other inorganic films on the surfaces of the metals). Although contact resistance is smaller compared to overall circuit resistance, it is an inseparable part of circuit resistance. Changes in the contact resistance may cause malfunctions or even major unwanted problems in the device. It has been stated in literature that the contact resistance can be reduced by producing electrical contacts that will create good metallic contact (thus modify contact force) or by designing a layout that will ensure that the contacts come together with a clean contact surface [31,34].

2.2.1.2. A-spot Temperature

Another important point to be considered about electrical contacts is temperature. Since electricity is transmitted only in a-spots (Figure 2.4), temperature rises in a-spots. It is also known that high contact resistance causes an increase in a-spots temperature. The temperature increasing in the contacts cause decreasing in current-carrying capacity of contacts. From another point of view, due to the nature of the a-spot clusters, the constriction resistance is not sensitive to small changes due to a-spot's size. However, when the contact resistance increases enough to increase local temperature (results with increasing in temperature), a self-accelerating deterioration will begin and the contact resistance will suddenly increase at the same time [31].

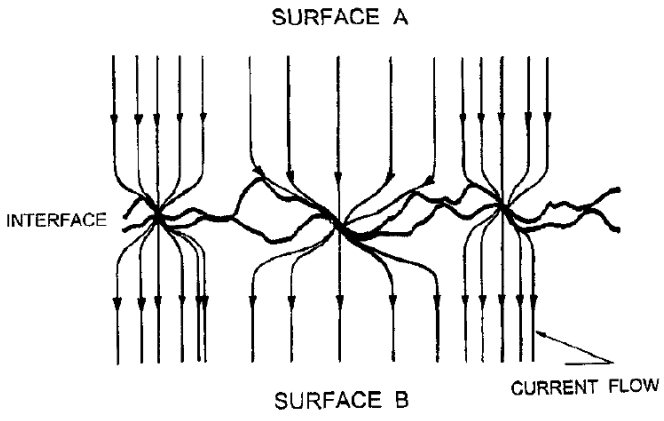

Figure 2.3 Illustration of current flow at contact interface [35].

2.2.1.3. Fretting

Another important issue to consider which occurs in contacts is fretting. Fretting occurs in four steps,

- the oxide film on the metal is broken due to mechanical action and metal comes out. This situation causes the metal to oxidize,
- adhesion wear, delamination and sheared micro-welds that occur in the asperities of the contact surfaces cause the material to be removed from the surface during contact,
- wear debris and hard abrasive particles continue to damage the contact surfaces,
- and based on the oxide layer and debris, a third body formation occurs between the contact surfaces. This situation occurring in the contact area causes a serious increase in contact resistance and consequently opens circuits.

2.2.1.4. High Erosion and Arcing

In a make/brake contact, when the current is above 0.1 A and the voltage is above a few hundred volts arc occurs. In an electrical system, an arc can be formed when the current is transmitted by non-conductive air. In make/brake contacts a series of events take place during contact of surfaces.

Making the Contact

The make/brake contacts have a breakdown voltage value. If the voltage exceeds this breakdown voltage value while the contacts are open, an electric field occurs and causes electron emission from the cathode. In the contact gap, the gas becomes ionized due to electron collisions and thus initiates the arc. As these occur, the current increases rapidly and the voltage required protecting the arc decreases. And as the contacts become closed, breakdown of contacts occurs at the separation of the contacts.

Breaking the Contact

When the make/brake contacts are opened during electricity transmission, the contact force which is applied to the contact surfaces decreases. Hence, the area of the a-spots decrease and the voltage drop increases. This causes the a-spot temperature rise and the contact surface to reach the melting point. As the distance between contact surfaces increases (contact gap increases) the molten metal forms a bridge. This molten metal releases its vapor into the contact gap. In this metal vapor (gas), ionization take place and it causes forming arc. As a result, breaking the contact occurs (Figure 2.5).

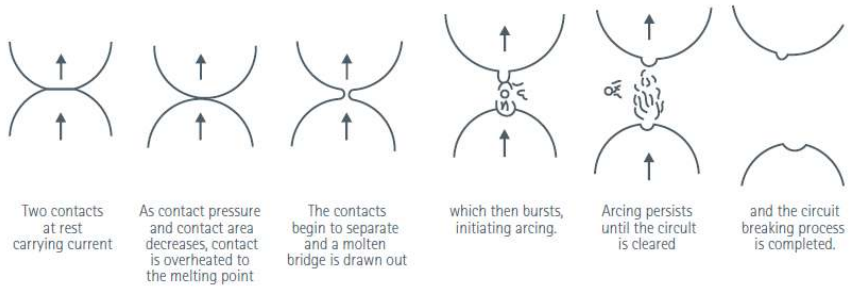

Figure 2.4 Breaking the contact [34].

The deterioration of the contact surfaces caused by the arc is important for electrical devices. In AC circuits, it is known that the arc can be extinguished by passing the current through zero in a well-designed contact test under suitable conditions. However, there is no natural current zero in DC circuits. For this reason, it has been stated in the literature that in order to ensure the zero current state in DC circuits, it is necessary to design the break so that the arc voltage is greater than the transient system voltage.

Welding

Welding in electrical contacts occurs in two different ways: dynamic and static welding. In dynamic welding, there is make-brake-make again (contact) state of the contacts. When the contacts are in the “make again contact” state, the molten metal regions that originate from the arc at the arc points cause welding between the contact surfaces (Figure 2.6).

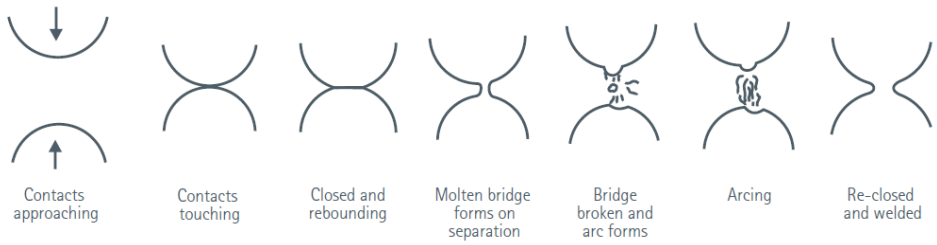

Figure 2.5 Illustration of dynamic welding on electrical contacts [34].

In static welding, welding occurs due to a short pulse but heavy current on the closed contact surfaces. High energy in small contact areas cause local melting in these regions and therefore welding on contact surfaces occur (Figure 2.7) [34].

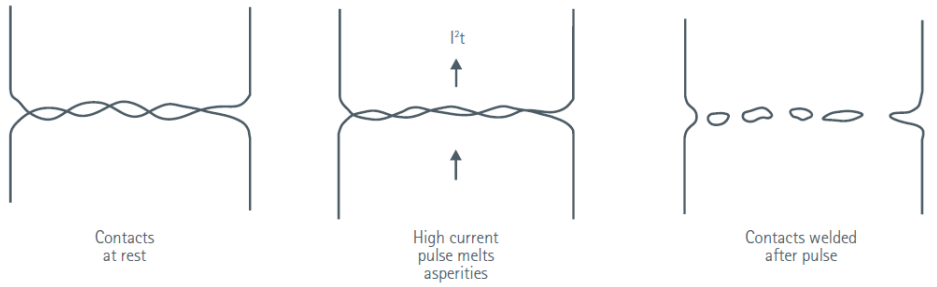

Figure 2.6 Illustration of static welding between electrical contact surfaces [34].

2.3. Electrical Contact Materials

The researches about electrical contacts go back to 1830s. The first paper about contacts written by Kohlrausch and Diesselhorst. Since then, many researches and investigations for the reliability of contacts have been made. Contact materials have been produced by using different methods and different materials in many studies due to minimize the effects of arc and welding in the contacts.

Lots of materials have been used in electrical contacts until now. And the most common pure materials used in electrical contacts are copper (Cu), silver (Ag), gold (Au), tungsten (W), platinum (Pt) and palladium (Pd). The copper and silver are the most used materials in electrical contacts (Figure 2.8). Cu is frequently used in electrical contacts thanks to its cheapness, alloying ability, high thermal and electrical conductivity properties etc. However, Cu and its alloys are prone to both corrosion and

oxidation. For this reason, electrical contacts are commonly protected by coating with materials such as Ag, Sn, Au, Pd and Ni or alloys of these materials [36-39].

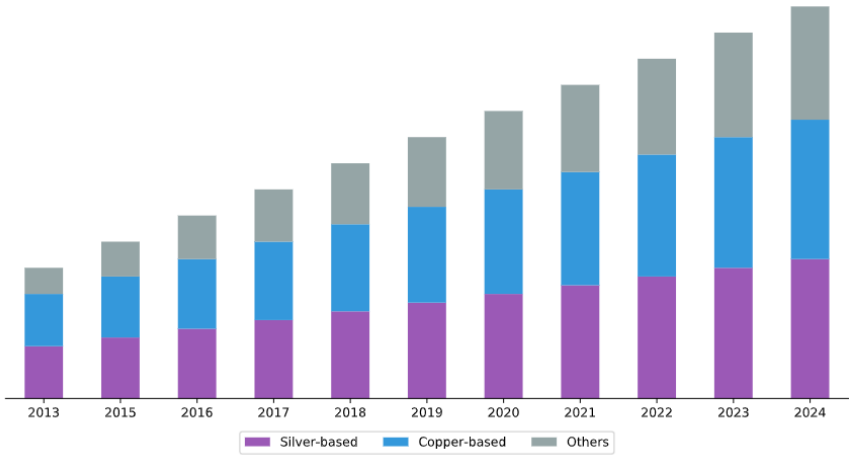

Figure 2.7 Global electrical contact materials market size, 2013-2024 (USD Million) [40].

The necessity of choosing a conductive material to obtain passage of electricity must be understood estimative. The duty of all of the electrical contacts is ensuring the passage of electricity without any interruption. At that point, the electrical contact materials must have properties such as;

- Good electrical conductivity,
- Constant contact resistance,
- Good thermal conductivity,
- Chemical stability,
- High wear resistance,
- High arc erosion resistance,
- High resistance against welding etc. [41,42].

2.3.1. Composite Electrical Contact Materials

Electrical contact materials must have the properties mentioned above in order to obtain safe and sufficient electrical transmission between contact pairs. It is impossible to obtain these properties at the same time with a pure material, and very difficult to obtain with an alloy. Therefore, composites have often been used in such applications to obtain global contact properties to achieve such properties [31]. Among composite materials, MMCs are the most commonly used composites for electrical contacts (because it is important that the matrix material should provide good thermal and electrical conductivity). The most commonly used MMC materials in electrical contacts can be listed as AgW, AgWC, CuW, AgC, AgMo, CuC and AgNi etc. [43].

Composites are unique materials that allow the development of the desired properties of the materials. And searching for new alternatives that help the development of composite systems is still continue. At this point, nanocomposites have become an alternative to deal with the limitations and are cited as the materials of the future.

2.3.2. Nanocomposite Electrical Contact Materials

Nanocomposite materials consist of at least one of the materials nano-sized in one, two or three-dimension, and as in composites, the material interfaces must be well defined. At the same time, matrix and reinforcement materials must be chemically inert to each other so that there will be no interaction between materials when one warms up until it melts. There are many advantages of nanocomposites compared to commercial composites such as high surface to volume ratio, better mechanical properties, improved optical properties, enhanced wear resistance, enhanced tensile and compressive behavior etc. [44-46].

Nanocomposites are divided into three different groups according to matrix material used,

- Ceramic Matrix Nanocomposites (CMNCs),
- Polymer Matrix Nanocomposites (PMNCs),
- Metal Matrix Nanocomposites (MMNCs) [45].

Metal Matrix Nanocomposites (MMNCs)

Among the composite materials, MMCs have gained a place in the aerospace and automotive industries with their properties such as high ductility, strength, toughness etc. Until the end of the 20th century, continuous and micron-scale discontinuous reinforcement materials were used with different metallic matrix materials to improve the properties of MMCs. However, the high cost and difficulties in synthesis have limited the use of continuous reinforced MMCs. Around year 2000, interest in nanomaterials increased and there was an interest in using nano-scale reinforcement with metallic matrices. MMCs reinforced with nanoparticles are called metal matrix nanocomposites (MMNCs). With the use of nanoscale reinforcement, interaction of the particles with dislocations becomes important in MMNCs, which allows improvements in mechanical properties compared to commercial MMCs [44,47]. Figure 2.9 shows the number of publications which are interested about MMNCs.

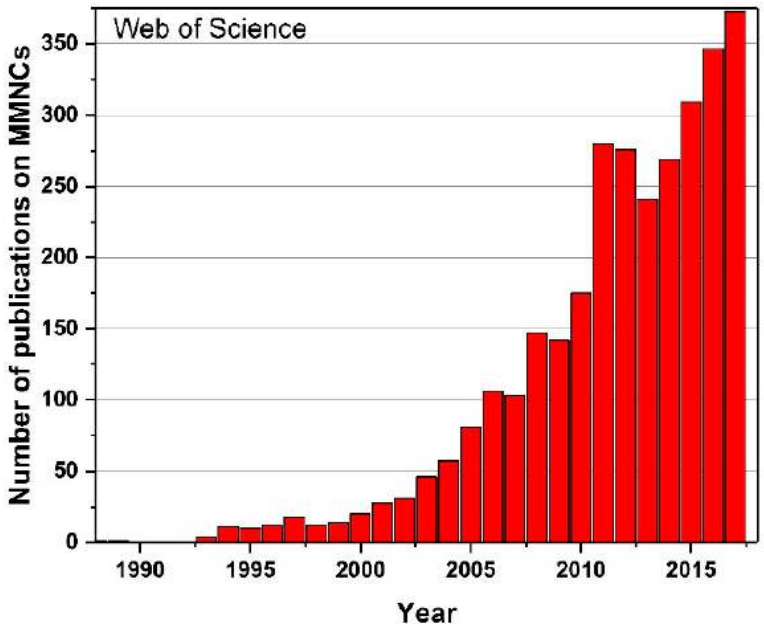

Figure 2.8 Number of publications about MMNCs in Web of Science [44].

MMNC materials are known to provide advantages over alloys. In the literature, it is stated that materials such as oxides, carbides, nitrides etc., several metals or alloys Si, Al, Ti, Zr can be reinforcement materials for MMNCs. As a result, MMNCs have been used in aerospace, automotive, electronics and military industries due to their high

mechanical properties, good electrical and thermal conductivity properties etc. [45,46]. Some common application area of MMNCs is given in the Table 2.1. Thanks to good electrical conductivity and good mechanical properties they provide, they are considered as electrical contact material in this study.

Table 2.1 Several common applications of MMNCs [45].

Nanocomposites	Application
Fe/MgO	Catalysts, magnetic devices.
Ni/PZT	Wear resistant and thermally graded coatings.
Ni/TiN, Ni/ZrN, Cu/ZrN	Industrial high speed machinery, optics and magnetic storage materials.
$Fe/Fe_{23}C6/Fe_3B$	Structural materials.
Cu/Al_2O_3	Electronic packaging.
Nb/Cu	Structural materials for high temperature applications

2.3.2.1. Electrical Nanocomposite Coating Matrix Materials

For the electrical industry, many metals had been used as matrix materials of coatings such as Cu, Ag and Au etc. It is stated in the literature that the basic elements for electrical contacts are Cu and Ag [36,43].

Copper

Good conductivity, thermal conductivity, low price properties of Cu makes this material a suitable choice for electrical contacts. It is generally used for high voltage connectors and oil circuit breakers. However, Cu based contacts have disadvantages such as short service life, inadequate contact performance, poor arc-extinguishing etc. Therefore, second phase addition is needed to improve reduce these disadvantages [36,48,49].

Silver

Ag is a soft, ductile, shiny metal with FCC structure. It is the highest electrically and thermally conductive material of all metals. These important advantages make this metal useful for electrical contacts and connector. However, at the same time, its drawbacks such as low corrosion resistance limits its usage in electrical industry. Literature advices adding a second phase to the electrical contact materials that will

prevent the deterioration of the contact surfaces due to arcing and improve the mechanical properties of the contact surfaces. Within this direction, silver and silver matrix composites are frequently used in the electronics industry due to their advantages properties such as high electrical conductivity, strength, crack resistance, and high wear resistance etc. To improve the properties of Ag electrical contact application, elements and their drawbacks is presented on the Table 2.2 [10,36,50-52].

Table 2.2 Effects of addition of some elements on properties of Ag [36].

Property	Additions
Arc resistance	Pb, Mg, Li, Zn, La, Sb
Abrasion resistance	Cu, Ni, Pd, Li
Lubrication	In, Zn, Sn, C
Weld resistance	In, Zn, Mn, metal oxides

Silver-based materials such as Ag-C, Ag-WC, Ag-Ni and Ag-ZnO have been frequently used in electrical contact materials. However, properties of these materials such as high contact resistance, serious material loss during contact, low welding resistance have created serious problems. Therefore, Ag-CdO electrical contact material has been used a lot due its excellent arc erosion resistance, low contact resistance, good welding resistance properties and it is named as “Universal Contact” in the past. Decomposition of CdO at high temperatures serves to absorb electric arc energy and Cd vapor helps to quench the arc. However, in addition to these advantages, it is a matter of question that Cd vapor and micro particles formed due to the arc can seriously harm the environment and people. Thus, developing a new reinforcement material for Ag matrix electrical contact is needed [7, 53-55]. Due to its being highest electrically and thermally conductive metal property, Ag is chosen as matrix material for this study.

2.3.2.2. Electrical Nanocomposite Coating Reinforcement Materials

Many materials such as Carbon Nanotubes, Graphene, SiC were used as reinforcement materials in composites. As can be expected from composites, these reinforcement materials do no blend with the matrix material neither in the solid nor in liquid states.

Carbon Nanotubes (CNTs)

CNTs are used commonly in biotechnology, electronics and nanotechnology due to their appropriate electrical, mechanical, and physical properties. They have unique properties such as high strength due to covalent bonds between each carbon atoms, high electrical conductivity, mobility etc. And because of their low-cost production methods, they are commonly used as reinforcement materials for composites. In addition, CNT reinforcement in coatings provide better wear resistance, microhardness and electrical properties.

Graphene (Gr)

Graphene is a nearly transparent, two-dimensional material and also strongest material ever tested according to the literature. Its thermal and electrical conductivity properties are efficient. Due to containing sigma and pi bonds, it conducts electricity gradually. And Gr was used as reinforcement material with matrix materials such as metals (Al, Cu, Mg, Ag), ceramic like materials (Si_3N_4, Al_2O_3, Zirconia) and polymers (PANI, PPS, PVA, PS, PET, etc.) successfully.

Silicon Carbide (SiC)

SiC is a material which have good mechanical properties and used as technically high-quality material. It is used in diodes, astronomy applications, heating elements etc. And they are also used as reinforcement materials in composites. It is an attractive material to use as a reinforcement material due to its high stiffness, high strength, low density properties etc. [43,56].

Titanium Diboride (TiB_2)

Titanium Diboride (TiB_2) is a ceramic material which is known by its stiffness and hardness properties. Since electrical and thermal conductivity is an important issue for electrical contact materials, TiB_2 is an excellent choice as reinforcement material. Because TiB_2 is electrically and thermally conductive material in contrast to most of ceramic materials [12].

Among the borides, TiB_2 is the highest boride elastic modulus, highest boride fracture toughness, highest boride compressive strength and second highest boride melting point [57]. The properties of monolithic TiB_2 compared to some metal borides are on the Table 2.3.

Table 2.3 Comparison of physical, mechanical and oxidation properties some metal borides [58].

Material	Crystal structure	Melting point (°C)	Density (g cm^{-3})	Co-efficient of thermal expansion (α; 10^{-6} K^{-1})	Thermal conductivity (W m^{-1} K^{-1})	Elastic modulus (GPa)	Hardness (GPa)	Fracture toughness (MPa m$^{1/2}$)	Flexural strength (MPa)	Oxidation resistance (°C)
TiB_2	Hex	3225	4.5	7.4	60–120	560	25–35	4–5	700–1000 (3-point)	<1200
HfB_2	Hex	3380	11.2	6.3	104	480	28	4	350–450 (4-point)	<1400
ZrB_2	Hex	3200	6.1	6.8	60–105	350	20–25	4	300–400	<1400
TaB_2	Hex	3040	12.5	8.2	16–35	550	25	4.5	555 (4-point)	<1400

TiB_2, is a hexagonal structure ceramic material known for its properties such as high hardness, high melting temperature, low density, low electrical resistivity, good thermal conductivity, good wear resistance, high oxidation resistance, high elastic modulus (Table 2.4). It is resistant to oxidizing atmosphere up to 1000°C. Thanks to these features, TiB_2 has been used in applications such as ceramic cutting tools, corrosion resistance parts, impact resistant armors, wear resistance coatings etc. [11,59-63].

Table 2.4 Values of some properties of TiB_2 [11,62].

Property	
Hardness	20-30 GPa (depending on applied load)
Melting Temperature	3498 K
Density	4495 kgm^{-3}
Electrical Resistivity	0.13 $\mu\Omega$m
Thermal Conductivity	37 to 122 Wm^{-1} K^{-1}, at 300 K
Elastic Modulus	>450 GPa

According to phase diagram in Figure 2.10, Ti and B are infinitely soluble in each other in liquid state and have no solubility in each other in solid state. The Ti-B system has three borides, TiB (18 wt% of B), Ti_3B_4 (22 wt% of B) and TiB_2 (30 wt% of B). TiB and Ti_3B_4 have an orthorhombic lattice, while TiB_2 has hexagonal lattice. It is also stated in the literature that TiB_2 is the most stable compound among Ti-B system compounds [64,65].

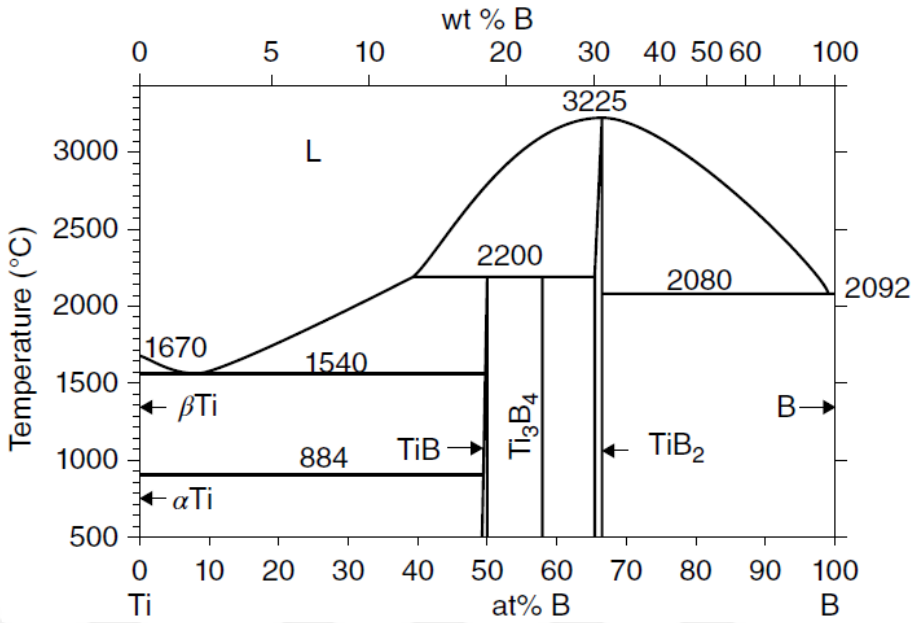

Figure 2.9 Ti–B binary equilibrium phase diagram [58].

The structure of TiB_2 can be described as stacking parallel B layers interbedded with hexagonal lattice of Ti (Figure 2.11). In this structure, each Ti atom is surrounded by 12 B atoms and each B atom is coordinated with 6 Ti atoms [11].

Metal matrices used with TiB_2 can be summarized as aluminum, $Al_{22}Fe_3Ti_8$, Fe, Ni, Cu and Ti etc. TiB_2 reinforcement is very useful in metal matrix composites. Because, metals generally have high thermal expansion coefficient (TEC) and limited stiffness and hardness. TiB_2 reinforcement causes decreasing in TEC while improving stiffness and hardness. Also, TiB_2 reinforcement reduces electrical and thermal conductivities less than other ceramic reinforcements compared to them [12]. Hence, it can be stated that TiB_2 is a potential reinforcement material for the nanocomposite coatings for electrical contacts.

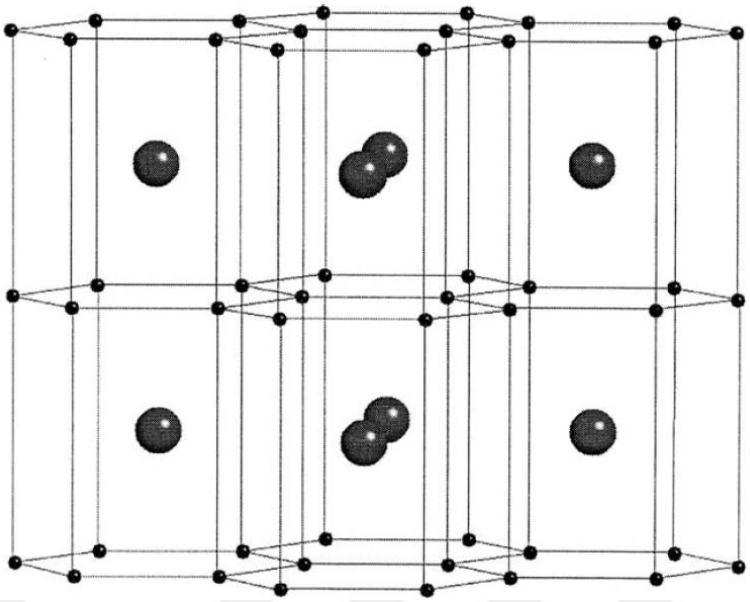

Figure 2.10 Crystal structure of TiB_2. Large and small spheres represent Ti and B atoms, respectively [11].

Also, it is stated in the literature that nanocomposites provide high surface to volume ratio, better mechanical properties, enhanced wear resistance, and enhanced tensile and compressive behavior compared to traditional composite coatings [45]. Consequently, nano TiB_2 reinforcement will be used in this study to improve these properties.

2.3.2.3. Fabrication Methods of Nanocomposite Coatings

Nanocomposite coatings are materials consisting of at least two phases which do not mix. These coatings must contain nanometer scale at least one dimension. Compared to conventional coatings, nanocomposite coatings show properties like higher hardness and heat resistance. It is also known that the movement of ions is restricted due to the presence of nanoparticles in nanocomposite coatings. It is also stated in the literature that these coatings can be produced cost-effectively without compromising its performance. It is expected that nanocomposite coatings are going to take place in more application fields in the future. Until today, many different coating production methods have been used to produce nanocomposite coatings. Examples of these methods are Sol-gel method, Cold Spray method, Chemical Vapor Deposition (CVD), Physical Vapor Deposition (PVD), Thermal Spray method, Dip Coating method, Electroless Deposition and Electrodeposition methods. Among all these methods, the

electrodeposition method draws attention with its advantageous features. Electrodeposition method has been used as nanocomposite coating production method in many studies in the literature [13,66].

Electrodeposition Method

Electrodeposition is a simple technique that requires a conductive surface (substrate to deposit) is immersed into an electrolyte which contains ions of metal to deposit, requires an electrical current for charge transfer reaction and film deposition on substrate [67]. Several nanostructured materials which may be produced by electrodeposition method are given in Table 2.5. The controllable potential applied causes control material formation process, over the microstructure and its properties. With such properties, electrodeposition is an extensively used method by researchers [68]. Figure 2.12 presents the electrodeposition system.

Table 2.5 Several types of nanostructured materials which may be produced by electrodeposition method [69].

Methods of electrodeposition	Types of nanostructure materials			
	Nanoparticles in a metal deposit	Nanomultilayers	Nanotubes/nanowires	Nanocrystalline materials
Direct current (DC)	Single metal deposit	Metal type 1 e.g. Ni layer	Nanotubes	Single metal
Pulsed direct current (PDC)	Nanoparticles			
Pulsed reverse current (PRC)	Alloy deposit		Nanowires	Alloy
Potentiostatic (P)		Metal type 2 e.g. Cu layer		
Pulsed potentiostatic (PP)	Multilayer deposit		Tree-like nanowires	Fe Co

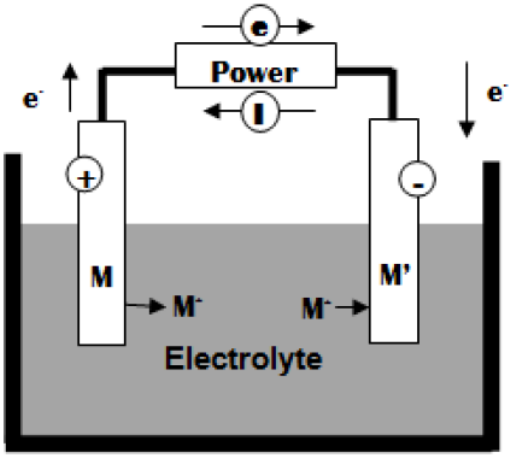

Figure 2.11 An illustration of electrodeposition set-up [70].

The substrate which is going to be deposited by nanocomposite coating has the duty of being cathode. The metal piece which is placed across the cathode in the electrolyte is anode. The electrolyte must contain metal salts and ions. The ions provide the flow of electricity in the electrolyte. The deposition process occurs mainly in a several steps,

- Current is given to the anode by power supply,
- atoms from anode oxidize and dissolve into electrolyte because of the applied current,
- electric current will be carried by positively charged ions from anode to the negatively charged cathode,
- thereby, metal ions which are in the coating bath (electrolyte) migrate toward extra electrons which are at near the cathode,
- finally, positively charged ions (from both bath content and anode) are reduced on surface of cathode (interface between electrolyte and cathode), therefore coating will be formed onto the surface of cathode.

And it must be stated that the thickness of the coating on substrate depends on the time duration of plating. Longer time for staying in chemical bath causes thicker coating on substrate [68,70,71].

During electrodeposition process, oxidation and reduction take place at the anode and cathode, respectively. These reactions occur because of the ions and electrons that can cross the electrode-electrolyte interface [72]. The oxidation and reduction reactions can be represented as;

Oxidation reaction; $X \rightarrow X^{z+} + ne^{-}$ **(2.1)**

Reduction reaction; $Y^{z+} + ne^{-} \rightarrow Y$ **(2.2)**

And, factors influencing electrodeposition process can be summarized as;

- Current density,
- Nature of anions or cations in the electrolyte,

- Bath composition,
- Temperature,
- Current waveform,
- Impurities,
- Nature of substrate surface [70].

Use of Different Current Types

Electrodeposition process can be obtained by using Direct Current, Pulse Current and Pulse Reverse Current methods. According to the applied current type, physical, mechanical and chemical properties such as deposition rate, grain structure will be changed. The traditional DC electrodeposition method is known mostly because of its being practical and easy to apply method for the deposition of pure metals, alloys and their composites. Moreover, in the recent years, PC and PRC electrodeposition techniques have been selected by researchers to investigate properties of composite coatings which are produced by electrodeposition method. These two deposition techniques provide different improvements on coatings such as higher deposition rate, better tribology properties, improved microstructural, mechanical and corrosion properties than the traditional DC method produced coatings. The current graphs of DC, PC and PRC methods are shown in Figure 2.13.

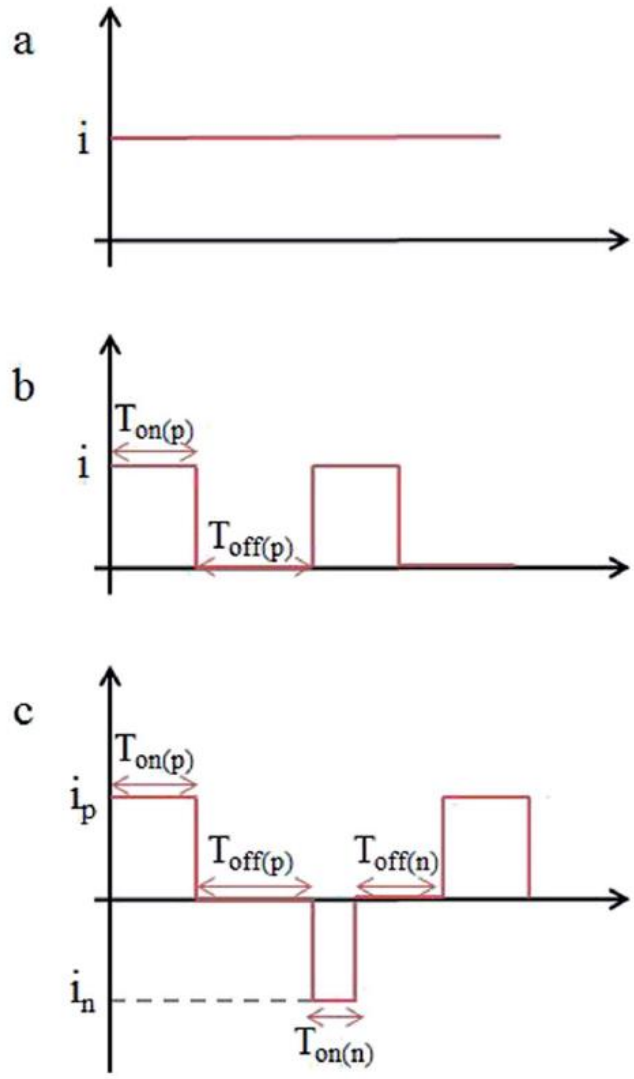

Figure 2.12 Schematic diagrams of DC, PC and PRC methods [73].

According to the studies in the literature, the PC method provides process parameters that are easier to control which resists to higher instantaneous current densities compared to traditional DC method. Therefore, it is stated in the literature that metal coatings which are deposited by PC method provide more unique compositions and microstructures than DC method. And in PRC method, there are two reaction processes, one is cathodic process (similar to PC method), other one is anode process which provides inhibiting grain growth and dissolving unsteady phases. It is highlighted in the literature that alloy coatings that are produced by PRC method

provides higher corrosion resistance and wear resistance compared to coatings produced by PC method [13,72-74].

Several advantages of PC and PRC methods are;

- Significantly increased limiting current density,
- More flexible process limitations,
- Improves uniform coating thickness,
- Provides coatings with finer grains (therefore lower stress and porosity occurs),
- Higher rate of deposition can be achieved to obtain better physical and mechanical properties [75].

Thus, the scope of this study is observing the effect of TiB_2 reinforcement in Ag matrix, amount of reinforcement and DC, PC and PRC current modes (which are used to produce nanocomposite coatings) on microstructural, mechanical and electrical properties.

2.4. Review of Related Works

Ag and Ag composite materials attract considerable attention for use in the electrical industry. And, in many studies in the literature, it is aimed to develop contact materials by adding a second phase to Ag composite coatings. In this section, several studies that are similar in terms of using the same raw materials, the same production method or same current types are reviewed.

L. Stappers et al. [76] produced Ag composite coatings co-deposited with carbon black nanoparticles by electrodeposition technique. Investigations showed that the current density and amount of particles in the solution significantly effects particle incorporation. It decreases with current density and increases with amount of particles. And it is found that the immobilization probability is less than 1. Contact resistance and wear tests of Carbon/Silver composite coatings were done during reciprocating fretting. Presence of carbon nanoparticles more than 9 vol% of coatings decreased friction coefficient (four times lower than pure silver coating), wear and contact

resistance. Also, less than 9 vol% of carbon black particles in coatings were resulted with contact resistance and friction coefficient results which are similar to pure silver coatings.

C. Shanthi et al. [77] studied silver plating on silver alloy by DC and Pulse plating methods. It was clearly observed that silver concentration (cathode) plays important role for amount of silver to be deposited on cathode. Therefore, higher silver purity provides higher silver deposition. The thickness of coatings produced by DC method was not uniform. Pulse plating was provided more uniform coating thickness compared to coatings produced by DC method. Also, less porosity and finer grains was observed for the coatings produced by Pulse plating method.

L. Al-Falahi et al. [43] produced unreinforced Ag and Ag-Gr nanocomposite coatings by using electrodeposition method with DC, PC and PRC methods. Besides the effect of Gr reinforcement in Ag matrix and current type on nanocomposite coatings, the effect of amount of Gr reinforcement in Ag matrix was also observed. The finer grain size were investigated in PC and PRC method deposited unreinforced Ag and high amount of Gr content of Ag-Gr coatings. The increased Gr content gave rougher surface because of the agglomeration. The Gr ratio was highest in nanocomposite coatings produced with PRC method compared to other nanocomposite coatings. And according to microhardness measurements, highest hardness value was belong to Ag-Gr nanocomposite coatings produced with PRC method. 10000 number of contact cycles were applied on all nanocomposite coatings. And contact resistance measurements of Ag coatings produced with DC, PC and PRC methods presented in Figure 2.14. Also, anti-erosion resistance of nanocomposite coatings was better than unreinforced Ag coatings in the light of electrical contact test results.

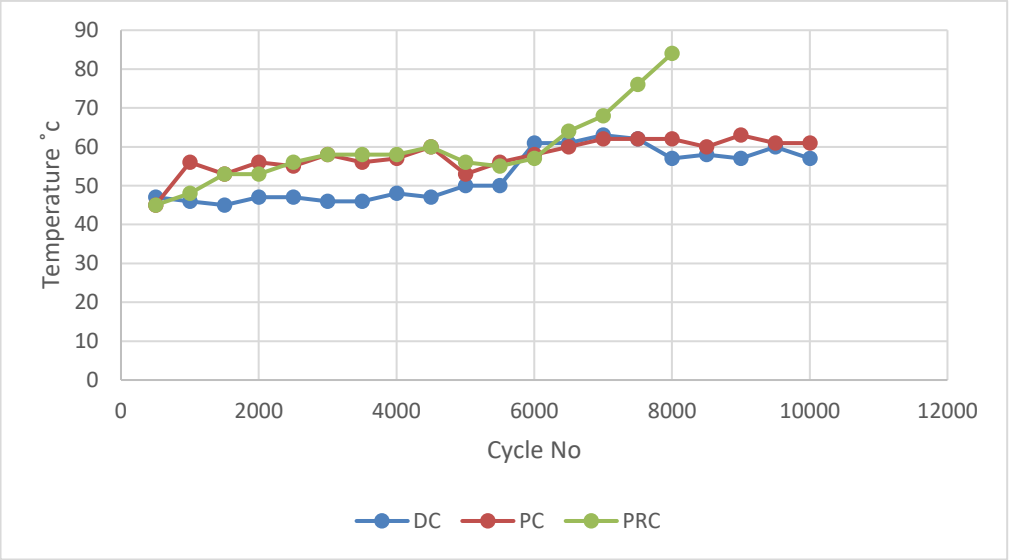

Figure 2.14 Electrical performance measurements of pure Ag coatings produced with DC, PC and PRC methods [43].

E. Gurcan et al. [56] achieved unreinforced Ag and Ag-SiC nanocomposite coatings on copper backings by electrodeposition technique with using DC, PC and PRC methods for electrical contacts. By using PC and PRC methods for electrodeposition process, more homogeneous coating surfaces were obtained. With these two methods, finer grain size and high amount of Si content in nanocomposite coatings were realized. Higher SiC content caused rougher coating surface. 4.0 g/L SiC reinforcement gave the highest coating surface roughness due to agglomeration. SiC reinforcement increased the hardness of coatings. The highest hardness value was obtained from Ag-SiC nanocomposite coatings which are reinforced with the amount of 1 g/L and deposited with PRC method electrodeposition due to less agglomeration and more homogeneous coating surface. Contact tests were applied on contact buttons up to 10000 number of contact cycle. And the temperature values during electrical contact performance tests of Ag-SiC nanocomposite coatings produced with DC, PC and PRC methods are presented in Figure 2.15.

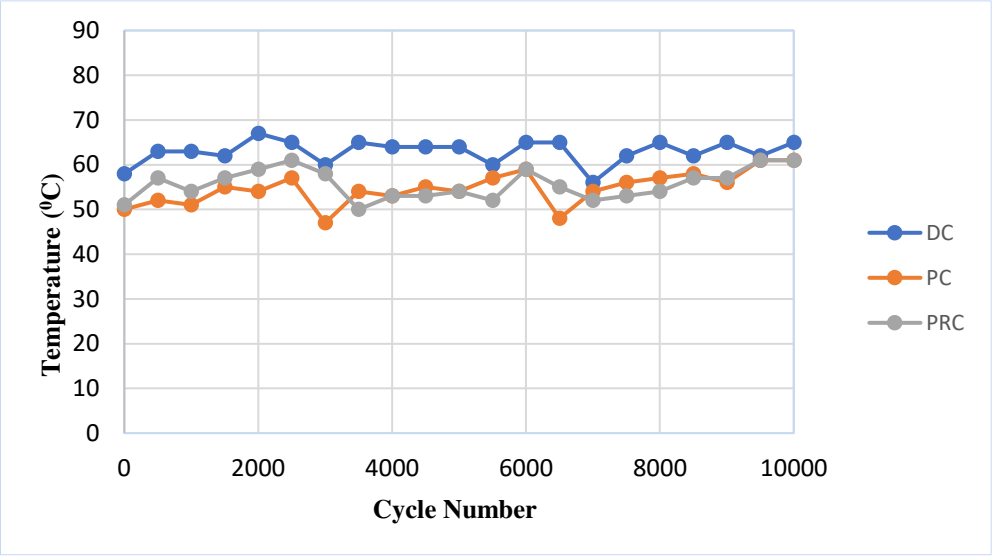

Figure 2.15 Electrical contact resistance analysis of Ag-SiC nanocomposite coating produced with DC, PC, PRC methods [56].

T. Borkar et al. [78] investigated pure nickel and nickel composite coatings (Ni–Al_2O_3, Ni–SiC, and Ni–ZrO_2) by electrodeposition technique with using DC, PC and PRC methods. They investigated that the PC and PRC method electrodeposition provided more weak crystallographic texture compared to DC method coatings. The improvements on microhardness and wear resistance were obtained on coatings produced by DC, PC and PRC methods for all nanocomposite coatings compared to pure nickel coatings. Different methods of electrodeposition changed surface roughness (Figure 2.16). Ni–Al_2O_3 nanocomposite coatings exhibited better microhardness and wear resistance than the Ni–SiC, and Ni–ZrO_2 nanocomposite coatings. Also, it is stated that increasing amount of Al_2O_3 content was resulted with the improving microhardness and wear resistance of nanocomposite coatings.

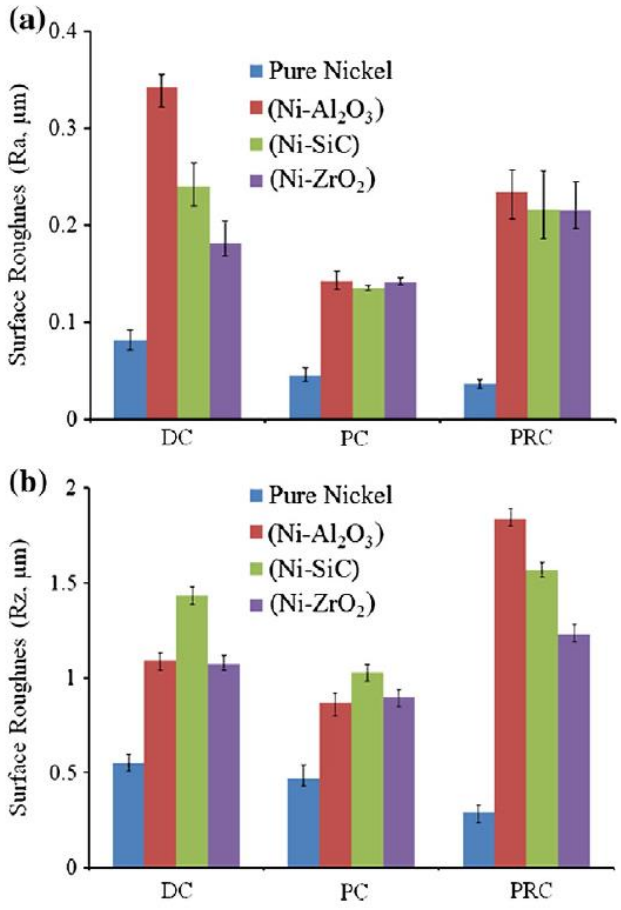

Figure 2.16 Surface roughness of nickel and nickel composite coatings deposited by DC, PC, and PRC electrodeposition methods: (a) Ra, and (b) Rz [78]. (Ra and Rz are surface roughness parameters)

H. Li et al. [79] investigated characteristics of Ag-TiB_2 contact materials. Effects of different Ni additions were estimated. Powder metallurgy was used as production method due to its being frequently used technique for composite contact materials. According to the results, they observed that the adding Ni and increasing the amount of it in Ag-TiB_2 composites results with decreasing in electrical conductivity and increases hardness. Among these contact materials produced with different amount of Ni, 2 wt% Ni added contact material showed least total mass loss and the optimal arc erosion resistance. The increasing hardness with the addition of Ni causes the reduce contact points which results with temperature increase short lasting time of molten bridge and break-arc-duration. Also, addition of Ni provides arc distinguishing at a

certain level. Therefore, excessive Ni addition in Ag-TiB_2 composites is not suitable for benefit of arc erosion resistance.

Y. XI et al. [80] studied on Ag based contact materials. They wanted to see the effect of contact force and electrode gap on material transfer. They were used arc erosion tests on Ag−4 wt.% TiB_2 contact material. The arc energy was decreased and then increased as the contact force increased (first increasing then decreasing were expected). Material transfer did not change, same mode takes place from anode to cathode. And the large electrode gap results with decreased make arc energy, and it does not effect on its distribution. In final, electrode gap effects material transfer from anode to cathode. The mass change of anode and cathode with respect to different electrode gaps is presented in Table 2.6.

Table 2.6 Mass change of anode and cathode of Ag−4 wt.% TiB_2 with respect to different electrode gaps [80].

Electrode gap/mm	Mass change/mg		Relative transfer mass/mg
	Anode	Cathode	
1	−1.30	+0.34	1.64
4	−0.12	−2.04	1.92

X. Wang et al. [81] aimed to investigate effect of TiB_2 particle size of Ag-TiB_2 nanocomposite for contact materials. Ag-4wt%TiB_2 nanocomposites which contain different TiB_2 particles was prepared by mechanical milling and powder metallurgy. The results show that smaller TiB_2 particles provide more uniform dispersion of reinforcement in Ag matrix (Table 2.7). Finer particle size was provided less mass loss and shorter arc duration. The leas mass loss and shortest arc duration results was belonged to composites which is prepared with 1.3 μm TiB_2 powder.

Table 2.7 Number of TiB_2 particles in each micro-area of composites prepared with different TiB_2 powders [81].

Number	Particle size/μm		
	6	2.8	1.3
01	72	450	461
02	108	469	493
03	105	463	471
04	85	470	464
05	115	455	492
06	96	443	480
07	120	485	490
08	117	462	474
09	123	487	462
S'_{rel}/%	17.21	14.78	12.99

And with the decrease in TiB_2 particle size, the erosion area of Ag-4wt%TiB_2 composites increases which demonstrates that the fine TiB_2 particle can improve arc erosion resistance of Ag-4wt%TiB_2 composites (Table 2.8).

Table 2.8 Erosion area of Ag-4wt%TiB_2 contact materials after vacuum arc erosion 50 times [81].

TiB_2 particle size/μm	6	2.8	1.3
Erosion area/mm^2	2.26	3.47	4.28

And surface morphologies of Ag-4wt%TiB_2 composites prepared with different powders are given in Figure 2.17. From the figure it can be stated that the smaller particle size of TiB_2 caused enlarging of the erosion area on nanocomposites.

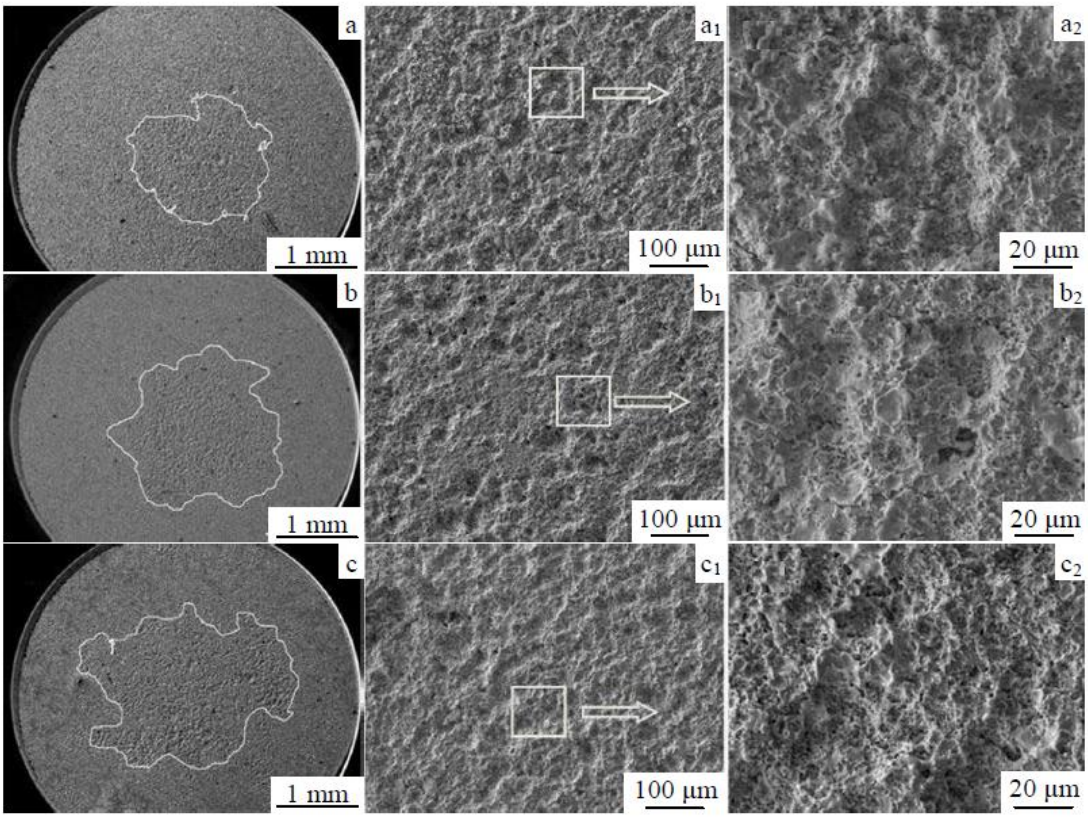

Figure 2.137 Surface erosion morphologies of Ag-4wt%TiB_2 composites prepared with different TiB_2 powders after arc erosion of 50 times at different magnifications: (a) 6 μm, (b) 2.8 μm, and (c) 1.3 μm [81].

CHAPTER 3

Experimental Procedure

3.1. Sample Preparation and Bath Composition

3.1.1. Sample Preparation

To obtain unreinforced Ag and Ag-TiB_2 nanocomposite coatings, both contact buttons and copper cylinders were used as substrates to deposition. Firstly, HDC6 contact buttons were removed from the contactors. The removed upper and lower contact buttons were had already basic coatings on copper backings. With the help of SiC papers with 600 grid, these coatings were removed and grinding was carried out so that the copper substrates were remained on contact buttons (Figure 3.1). The smoothness of the copper substrates for deposition process was provided with the help of grinding process. Before the deposition process, other parts of the contact buttons were painted with a non-conductive paint so that the surfaces to be deposited remain open. Thus, it was ensured that only desired area will be deposited on contact buttons. And after cleaning with distilled water and drying with a drier, the substrates were ready for deposition process.

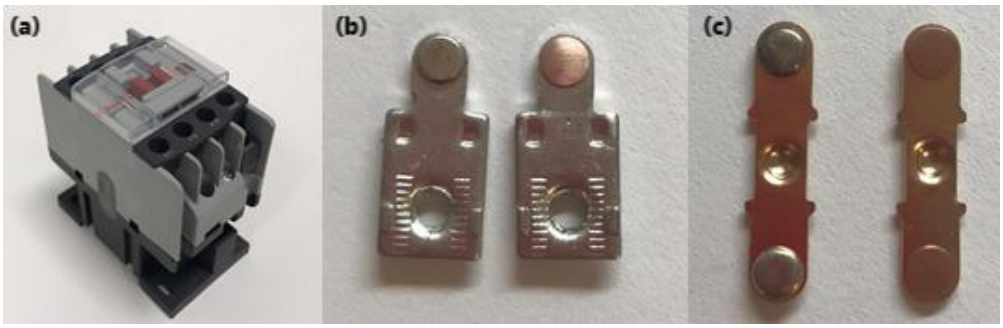

Figure 3.1 (a) An HDC6 contactor of Himel brand, (b) upper HDC6 contact buttons, (c) lower HDC6 contact buttons before and after grinding process.

The unreinforced Ag and Ag-TiB_2 nanocomposite coatings produced on copper backings on the contact buttons were also produced on copper cylindrical surfaces. These copper cylindrical substrates were cut from a hot rolled copper rod with a

diameter of 8 mm and a length of 3 mm by using BUEHLER Iso Met Low Speed Saw machine. The reason why the same depositions were also produced on copper cylinders is that the contact surfaces of the buttons are too small and are not suitable for analyzes such as hardness, XRD etc. Therefore, copper cylinders were subjected to be deposited with unreinforced Ag and Ag-TiB_2 nanocomposite coatings. Before deposition process, the copper cylinders were brazed with a cable from back (to immerse in the electrolytic bath easily), grinded by SiC papers with 600 grid for cleaning and becoming smoother of the substrates, and painted with the non-conductive paint so that the surfaces to be coated remain open (Figure 3.2). After painting, the areas to be deposited were cleaned with distilled water and dried with a drier before deposition process.

Figure 3.2 A copper cylinder prepared for the deposition process.

3.1.2. Bath Composition

After optimizing procedures of electrodeposition, mainly, two different kind of deposition baths were used to obtain unreinforced Ag and Ag-TiB_2 nanocomposite coatings onto copper substrates. Unreinforced Ag electrolytic bath was contained 10g/L Silver Nitrate ($AgNO_3$), 10g/L Potassium Cyanide (KCN) and distilled water (balance). Silver Nitrate is the source of silver ions and Potassium Cyanide has the duty of dissolving Silver Nitrate.

In order to determine the composition of the Ag-TiB_2 nanocomposite electrolytic bath, preliminary studies have been carried out for the surfactant to be used primarily. The task of a surfactant is to prevent the nanoparticles in the bath from agglomeration and forming inhomogeneity. Thereby, Ag-TiB_2 nanocomposite electrolytic baths were obtained by using different amounts of two different surfactants, Sodium Dodecyl Sulfate Salt (SDS) and Hexadecyltrimethylammonium Bromide (CTAP) for comparison. The desired homogeneous electrolytic bath was carried out with the Ag-TiB_2 nanocomposite electrolytic bath produced with using 0.2 g/L SDS. And, in order to examine the effect of using different amounts of nano TiB_2 on nanocomposite coatings, TiB_2 was used in 0.5, 1.0, 2.0 and 4.0 g/L quantities in the electrolytic baths. Thus, the optimum electrolytic bath obtained in line with the preliminary studies is given in the Table 3.1. Also, the pH values of the unreinforced Ag and Ag-TiB_2 nanocomposite electrolytic baths were measured as 11.

Table 3.1 Bath composition of Ag-TiB_2 nanocomposite coatings.

MATERIAL	QUANTITY
Silver Nitrate ($AgNO_3$)	10 g/L
Potassium Cyanide (KCN)	10 g/L
Sodium Dodecyl Sulfate Salt (SDS)	0.2 g/L
Titanium Diboride (TiB_2)	0.5, 1.0, 2.0 and 4 g/L
Distilled Water	Balance
Total	**50 L**

3.2. Electrodeposition Process

During preliminary studies, it was observed that mixing Ag-TiB_2 nanocomposite electrolytic baths with an Ultrasonic Homogenizer before deposition process, helps the formation of homogeneous deposition surface. Therefore, the Ag-TiB_2 nanocomposite electrolytic baths were mixed with an Ultrasonic Homogenizer (Figure 3.3) during preliminary studies with different mixing times. After analyzing depositions whose coating baths were mixed with the Ultrasonic Homogenizer with different times (15, 30, 45 and 60 minutes) before deposition process, it was seen that the 30 minutes is enough for the homogeneously dispersion of particles in the baths. Thus, all of the

nanocomposite electrolytic baths were mixed for 30 minutes by Ultrasonic Homogenizer before electrodeposition process.

Figure 3.3 Ultrasonic Homogenizer.

Electrodeposition method was used as the coating method during this study. This method was preferred due to its advantageous properties such as being cheap and easy to apply method. After mixing by Ultrasonic Homogenizer, the coating baths were taken onto a magnetic stirrer for deposition. After mixing in homogenizer, temperature of coating baths was very high (85 ° C). Therefore, before deposition, baths were kept in the magnetic stirrer for a while for reducing and stabilizing the temperature. After bath temperature reaches 55±5 °C, the deposition set-up (anode-cathode) was prepared inside the coating bath. As it was mentioned in the literature review, the surfaces to be deposited of substrates were immersed in the bath, face to face with the silver ingot. Thereby, the silver ingot has the duty of being anode, copper cylinders and contact buttons have the duty of being cathode during electrodeposition processes. The silver ingot was 5 g in weight and dimensions of it was 1 cm in width, and 2 cm in length. And it must be stated that the silver ingot acts as a silver ion source, not only Silver Nitrate in the coating bath. Electrodeposition process took place with a Barakuda electroplating device. With this device, using different current types became possible during this study. The bath was kept at an average temperature of 55±5 °C and mixed at 150 rpm by a magnetic stirrer during deposition process. In addition, coatings produced by different current types were analyzed and optimum values for deposition

process were determined. In preliminary studies with DC, PC and PRC methods, it was observed that the average current density of 10 mA and the coating time of 120 minutes was sufficient for the desired 40-50 micron coating thickness. And it must be stated that the unreinforced Ag and 0.5, 1.0, 2.0 and 4.0 g/L reinforced nanocomposite coatings were produced only by DC, 1.0 g/L reinforced Ag-TiB_2 nanocomposite coatings were also produced by PC and PRC electrodeposition methods during this study. Graphs of the current types which had been clarified in line with the preliminary studies are given in the Figure 3.4. Current density for DC method was 10 mA during deposition process. T_{on} and T_{off} values were 20 and 0 mA for PC method deposition, respectively. And in PRC method deposition, 40, 0 and -10 mA for T_{on}, T_{off} and anodic T_{on} (reverse T_{on}) were used respectively.

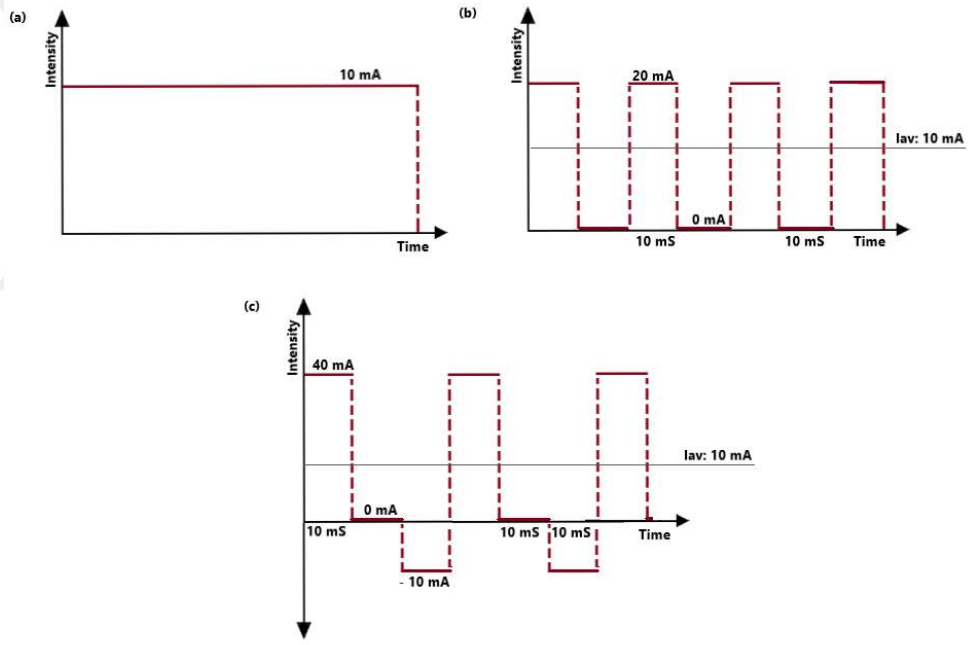

Figure 3.4 Graphs of (a) direct current, (b) pulse current and (c) pulse reverse current methods.

With the accordance of Figure 3.4 and in the light of equation 3.1, the duty cycles are calculated as 100%, 50% and 33.3% for DC, PC and PRC methods, respectively. T_{on} is on time and T_{off} is off time of pulse cycles.

$$\text{Duty Cycle} = T_{on} / (T_{on} + T_{off}) \quad \textbf{(3.1)}$$

Thus, unreinforced Ag and Ag-TiB_2 nanocomposite coatings were produced by electrodeposition method on contact buttons and copper cylinders with an average current of 10 mA and deposition time of 120 minutes. In this study, the effects of TiB_2 reinforcement into Ag matrix, reinforcement amount and current type in nanocomposite depositions on properties such as microstructure, hardness, contact performance, surface morphology will be examined.

3.3. Characterization Methods

3.3.1. Scanning Electron Microscope (SEM) Analysis

In order to get information about the topography and composition of the produced coating surfaces, analyzes were made with Scanning Electron Microscopy (SEM). HITACHI SU5000 Field Emission Scanning Electron Microscope (FE-SEM) device was used for this purpose which is shown in Figure 3.5. SEM analysis of all produced unreinforced Ag and Ag-TiB_2 nanocomposite coatings on electrical contact buttons were performed before and after electrical contact tests.

Figure 3.5 HITACHI SU5000 Field Emission Scanning Electron Microscope (FE-SEM) with the Energy Dispersive Spectroscopy (EDS) detector.

3.3.2. Energy Dispersive Spectroscopy (EDS) Analysis

Energy Dispersive Spectroscopy (EDS) analysis were also used on all unreinforced Ag and Ag-TiB_2 nanocomposite coatings on contact buttons in order to get information about elemental analysis. The SEM with an EDS detector which is shown in Figure 3.5 was used for EDS analysis of depositions. It must be stated that the EDS analyzes were obtained from deposited electrical contact buttons before and electrical contact tests.

3.3.3. X-Ray Diffraction (XRD) Analyzes

Due to the small diameter of the coatings on the contact buttons (4mm in diameter), same coatings were also produced on copper cylinders (8mm in diameter) in order to perform analyzes such as X-Ray Diffraction (XRD). Information about the crystallographic structures of these coatings was obtained by XRD analysis with using RIGAKU Miniflex600 generator which is shown in the Figure 3.6. The XRD analyzes were performed on unreinforced Ag and Ag-TiB_2 nanocomposite coatings by using CuKα radiation with the wavelength of 1.54059 Aº. Also, the scanning took place with 2 degrees per minute and the 2θ range was between 35° and 85°. Thereby, the effects of nano TiB_2 reinforcement, amount of reinforcement and different current types on nanocomposite coatings on crystallographic structure were observed.

Figure 3.6 X-Ray Diffraction (XRD) instrument.

3.3.4. Hardness Measurements

The hardness tests were obtained on cross-section of coatings which are deposited on copper cylinders. SHIMADZU HMV-G micro Vickers hardness device was used for hardness measurements (Figure 3.7). Five measurements were taken from different points of every substrate. Because measurements are taken more than once and averages of measurements must be calculated due to obtain more accurate results. The Vickers Hardness test procedure consists of indentation by a diamond indenter and measuring the size of it. Force is generally applied for 15 second and the indentation size is measured with a microscope. Larger indentation means softer test material. The diamond recess has a pyramid shape with an angle of 136 °.

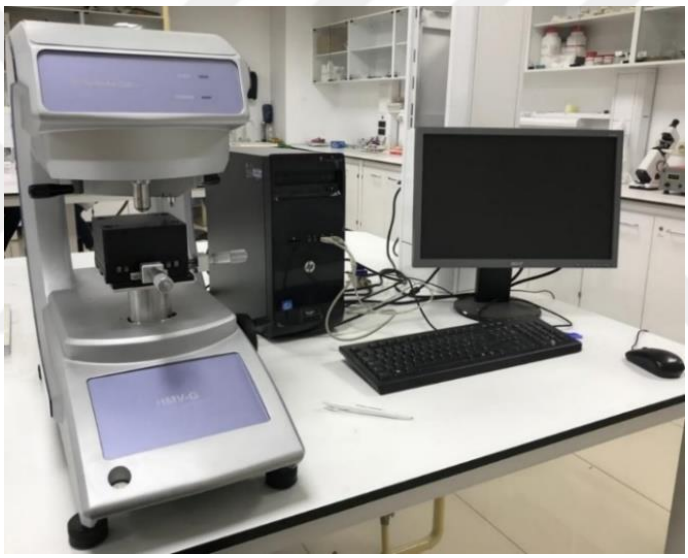

Figure 3.7 SHIMADZU HMV-G micro Vickers hardness device.

3.3.5. Coating Thickness Measurements

The deposited cylindrical samples were cut with Low Speed Saw apparatus from intersect. One side of every sample were mounted with Bakelite by using hot mounting machine for obtaining thickness of coatings. After mounting step, the grinding process took place by using SiC papers with the grade sizes of 400, 600, 800, 1000 and 1200. After that, sample surfaces were polished with a 3 μm diamond suspension on the MD Mol for getting mirror like view. And the prepared samples were analyzed with SEM

in order to get information about growth of coating and measure the coating thickness from cross-section.

3.3.6. Electrical Resistivity Measurements

Two-point electrical resistivity testing method was used to obtain electrical resistivity measurements which are done on coatings deposited on copper cylindrical substrates. Resistivity (R) values were measured according to the voltage (V) and current (I) measurements.

3.3.7. Arc Erosion Morphology

Contact test is necessary for the characterization of chemical effects such as melting, arc erosion, and welding on contact surfaces. Therefore, unreinforced Ag and all Ag-TiB_2 nanocomposite coatings on contact buttons were analyzed with SEM after electrical contact tests due to observing chemical effects of contact on coating surfaces.

Contact tests were applied on coatings which are deposited on copper backings of contact buttons. A hand-made electrical contact test mechanism (Figure 3.8) was prepared and used to perform contact tests for electrical contact buttons in Ankara Yıldırım Beyazıt University. An illustration of contact test which is used during this study is given in Figure 3.9. During the contact tests, the temperature on the contact buttons was transferred to the computer via Arduino and a program to record the exact values. The program which was used for recording the temperature values during contact test is given in the Appendices. The contact tests were took place at a constant load of 4 kW with a ~18 A /DC current and voltage of 220 V.

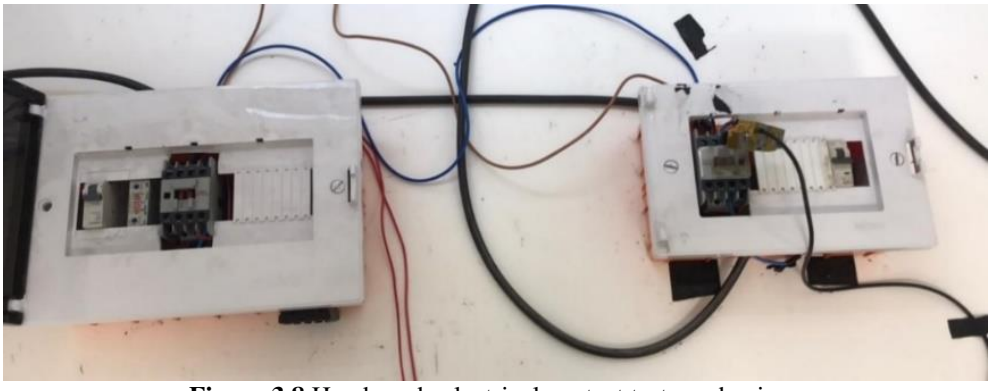

Figure 3.8 Hand-made electrical contact test mechanism.

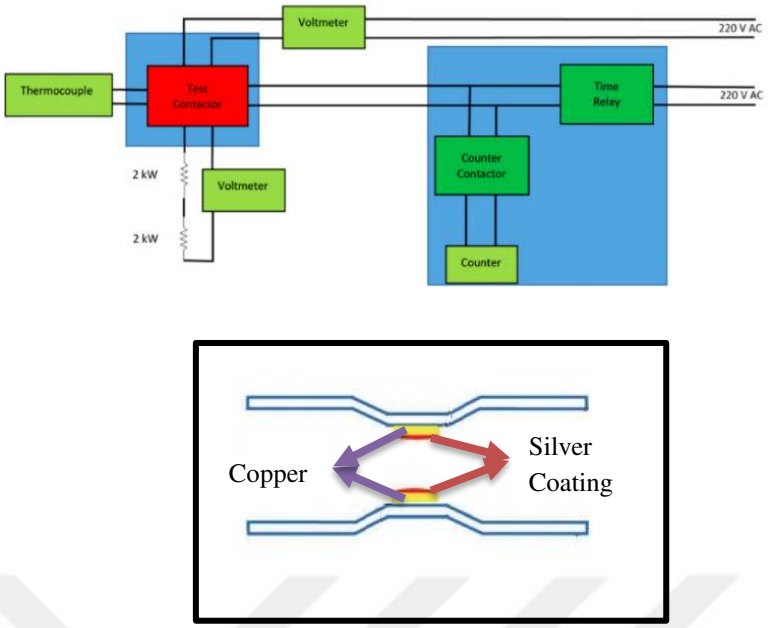

Figure 3.9 An illustration of contact test set-up which is also used during this study [43].

3.3.8. Corrosion Resistance Tests

Corrosion resistance tests were done on unreinforced Ag and Ag-TiB_2 nanocomposite coatings which are deposited on copper cylinders. A Ch Instruments electrochemical workstation device (Figure 3.10) was used for corrosion resistance tests. The tests were taken place with % 3.5 NaCl solution. The corrosion experiments were represented with Tafel plots for this study. The tafel plot paremeters used in corrosion tests are represented in Table 3.2. By comparison, the effect of TiB_2 reinforcement, amount of reinforcement and type of current on nanocomposite deposotions on corrosion resistance properties were determined.

Figure 3.7 Corrosion resistance test equipment including Ch Instruments Electrochemical workstation device.

Table 3.2 The Tafel plot paremeters used in this study.

Initial E (V)	-1
Final E (V)	1
Sweep Segment	1
Hold Time at Final E (s)	0
Scan Rate (V/s)	0.0005
Quiet Time (sec.)	2
Sensitivity (A/V)	$1x10^{-2}$

CHAPTER 4

Results and Discussion

4.1. Structural Analysis Before Contact Test

4.1.1. Microstructural Analysis

SEM analyzes were performed to obtain detailed information about surface morphologies of the unreinforced Ag and Ag-TiB_2 nanocomposite coatings produced on contact buttons. Low magnification SEM images of unreinforced Ag and 0.5, 1.0, 2.0 and 4.0 g/L Ag-TiB_2 nanocomposite coatings produced with DC method are presented in Figure 4.1. It can be clearly seen that addition of nano TiB_2 into electrolyte significantly changed the surface morphology of deposits.

According to SEM images which are performed with higher magnification (Figure 4.2), it is observed that the TiB_2 caused change in coating surface morphologies including surface homogeneity and surface roughness with the increased amount of nano TiB_2 added into electrolyte. First, big particles are observed on surface of unreinforced Ag coating. With introducing nano TiB_2, particles become smaller because of the reinforcement. And with the increased nano TiB_2 addition into electrolyte, these particles become smaller and more flat coating surface is observed (Figure 4.2 (c)). It can be stated that the incorporation of nano TiB_2 decreased roughness due to grain refining resulted with the smaller particles. Homogeneity and dispersion were increased due to grain refining. But addition above 1.0 g/L nano TiB_2 into electrolyte caused coarser particles due to agglomeration and coating surface become less flat and compact with the increased roughness. In the light of these considerations, the most homogeneous, flat and compact coating surface with smaller particles was observed with 1.0 g/L Ag-TiB_2 nanocomposite coating among these five coatings.

Composition of Coating	Coatings Produced with DC Method
Unreinforced Ag coating	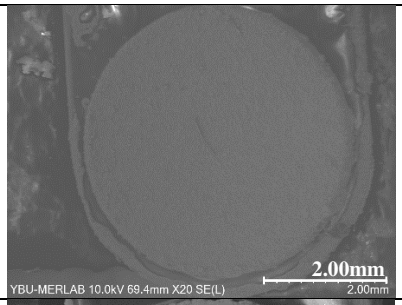
0.5 g/L reinforced Ag-TiB_2 nanocomposite coating	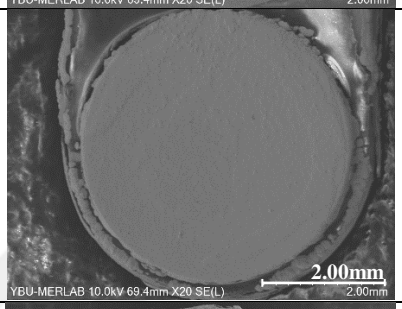
1.0 g/L reinforced Ag-TiB_2 nanocomposite coating	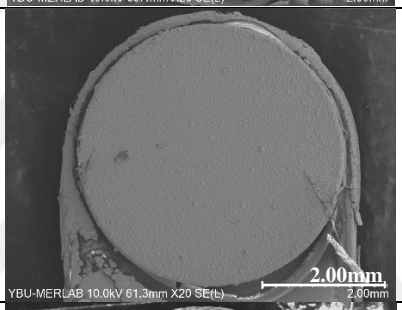
2.0 g/L reinforced Ag-TiB_2 nanocomposite coating	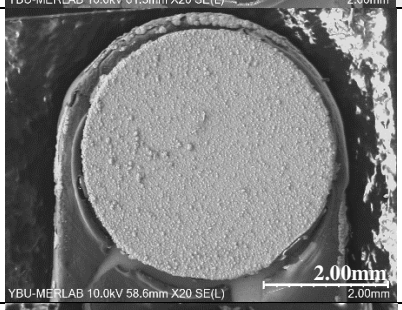
4.0 g/L reinforced Ag-TiB_2 nanocomposite coating	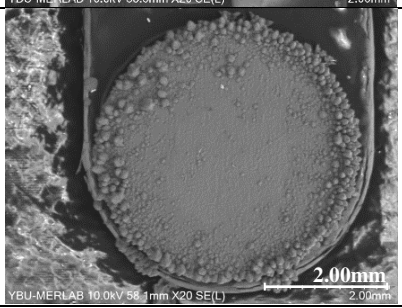

Figure 4.1 Low magnification SEM images of unreinforced Ag and Ag-TiB_2 nanocomposite coatings deposited by DC method electrodeposition.

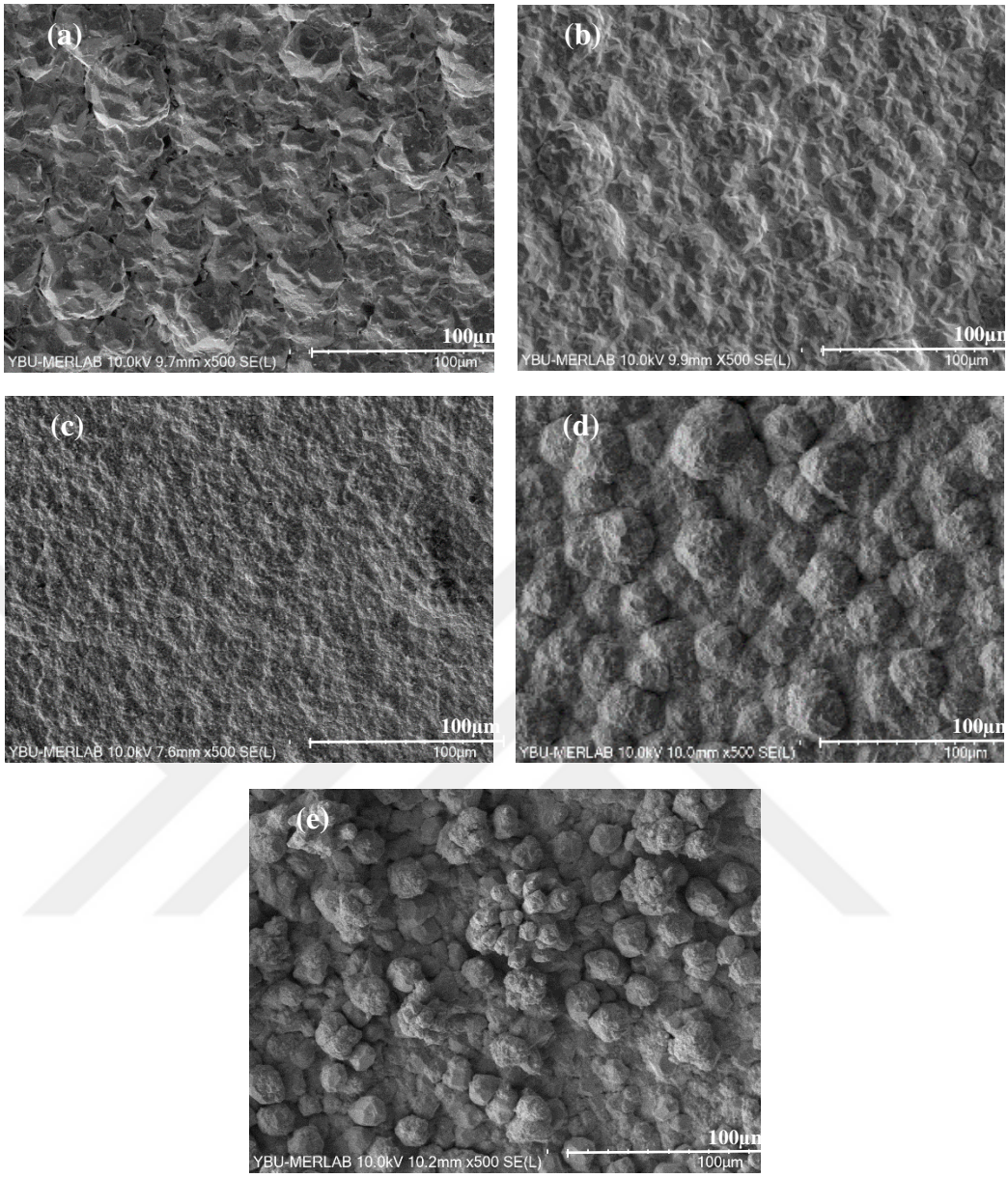

Figure 4.2 SEM images of (a) unreinforced Ag and (b) 0.5, (c) 1.0, (d) 2.0 and (e) 4.0 g/L Ag-TiB_2 nanocomposite coatings deposited by DC method.

In order to observe the effect of current type on Ag-TiB_2 nanocomposite coatings, 1.0 g/L Ag-TiB_2 nanocomposite coating was also produced by using PC and PRC methods. Low magnification SEM images of 1.0 g/L Ag-TiB_2 nanocomposite coatings produced via DC, PC and PRC methods are presented in Figure 4.3.

Composition and Current Type of Deposition	1.0 g/L Reinforced Ag-TiB_2 Nanocomposite Coatings
1.0 g/L reinforced Ag-TiB_2 nanocomposite Coating by DC method	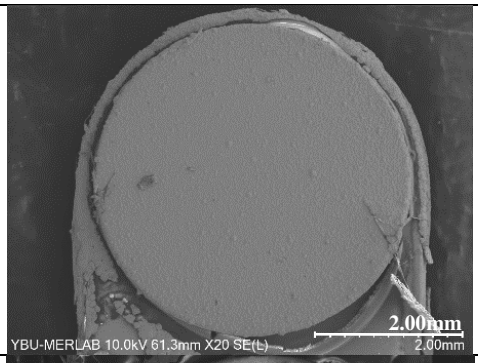
1.0 g/L reinforced Ag-TiB_2 nanocomposite Coating by PC method	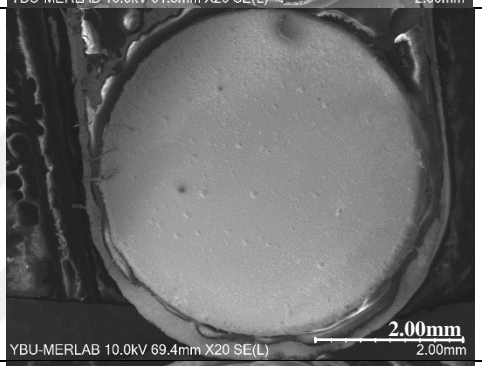
1.0 g/L reinforced Ag-TiB_2 nanocomposite Coating by PRC method	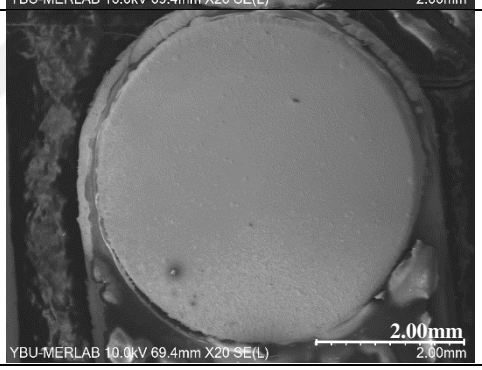

Figure 4.3 SEM images with low magnification of 1.0 g/L Ag-TiB_2 nanocomposite coatings deposited by DC, PC and PRC method electrodeposition.

In order to analyze surface morphologies of these three coatings, SEM images were also examined with higher magnification (Figure 4.4). Homogeneous and flat coating surface is obtained with 1.0 g/L Ag-TiB_2 nanocomposite coating produced by DC method. And with the PC and PRC methods, coarser particles on coatings surface is observed because of volume increase which resulted by nano TiB_2 reinforcement into Ag matrix. Despite of this situation, still homogeneous and flat surface is present due to grain refining of Ag matrix with using PC and PRC methods. Therefore, it can be

stated that PRC method helps the formation of uniform and flat structure despite of volume increase due to nano reinforcement into matrix.

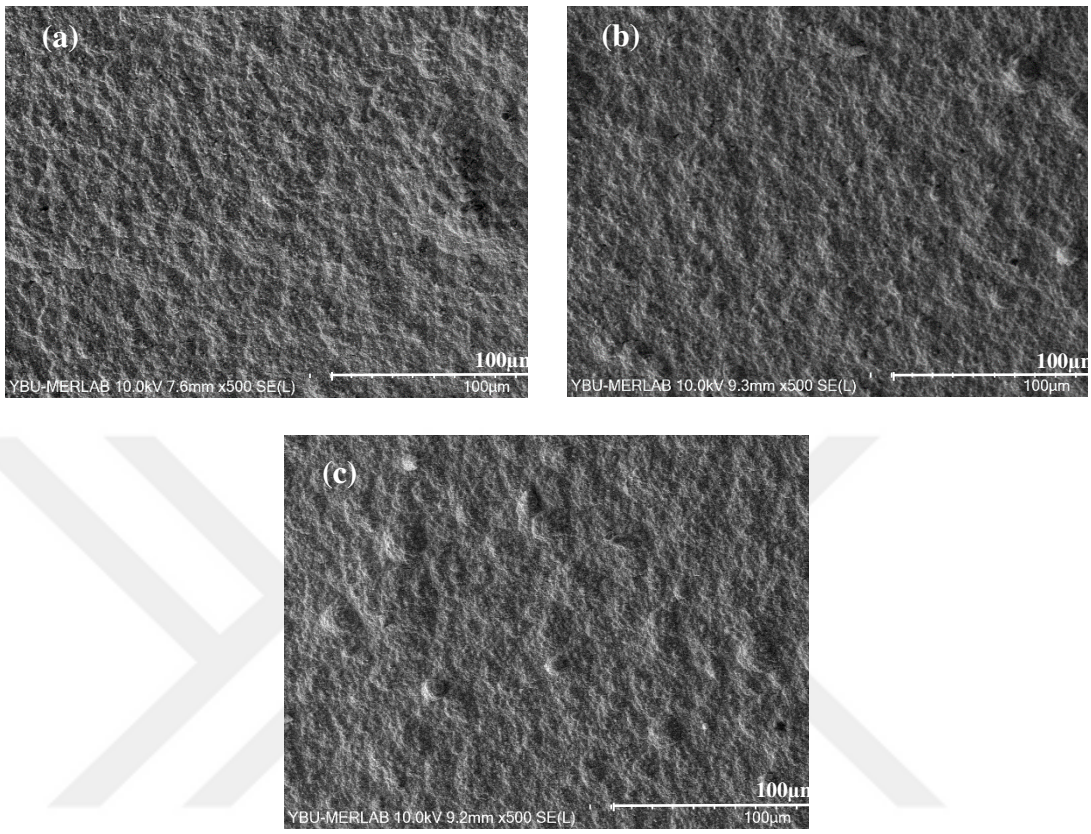

Figure 4.4 SEM images of 1.0 g/L Ag-TiB_2 nanocomposite coatings deposited by (a) DC, (b) PC and (c) PRC method electrodeposition.

4.1.2. Energy Dispersive Spectrometer (EDS) Analysis

The elements and their ratio of unreinforced Ag and Ag-TiB_2 nanocomposite coatings deposited on contact buttons are investigated by using Energy Dispersive Spectrometer (EDS). The EDS map sum spectrum of unreinforced Ag produced by DC electrodeposition method is given in Figure 4.5.

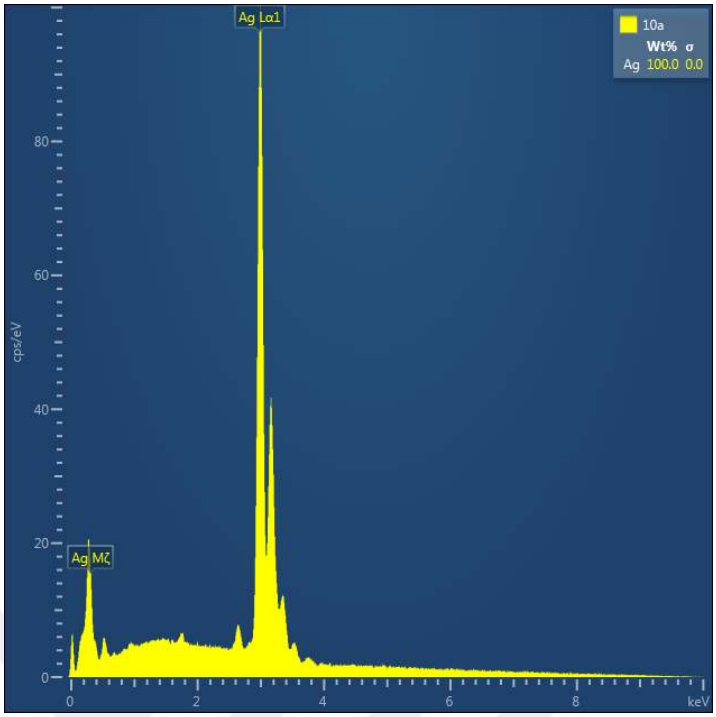

Figure 4.5 EDS map sum spectrum of unreinforced Ag coating produced by DC electrodeposition method.

Comparison of Ti wt% of 0.5, 1.0, 2.0 and 4.0 g/L Ag-TiB_2 nanocomposite coatings produced with DC method is presented in Figure 4.6. According to the EDS analysis, as amount of nano TiB_2 added into electrolyte increased, ratio of Ti in deposits are increased too. Therefore, the highest Ti wt% was obtained with 4.0 g/L Ag-TiB_2 nanocomposite coating (0.8 wt%) among four nanocomposite coatings. Eslami et al. [82] studied Cu-Si_3N_4 composite coatings produced by DC method electrodeposition. Similarly, they investigated that increased Si_3N_4 concentration into electrolyte caused increasing Si_3N_4 particles in deposited layer.

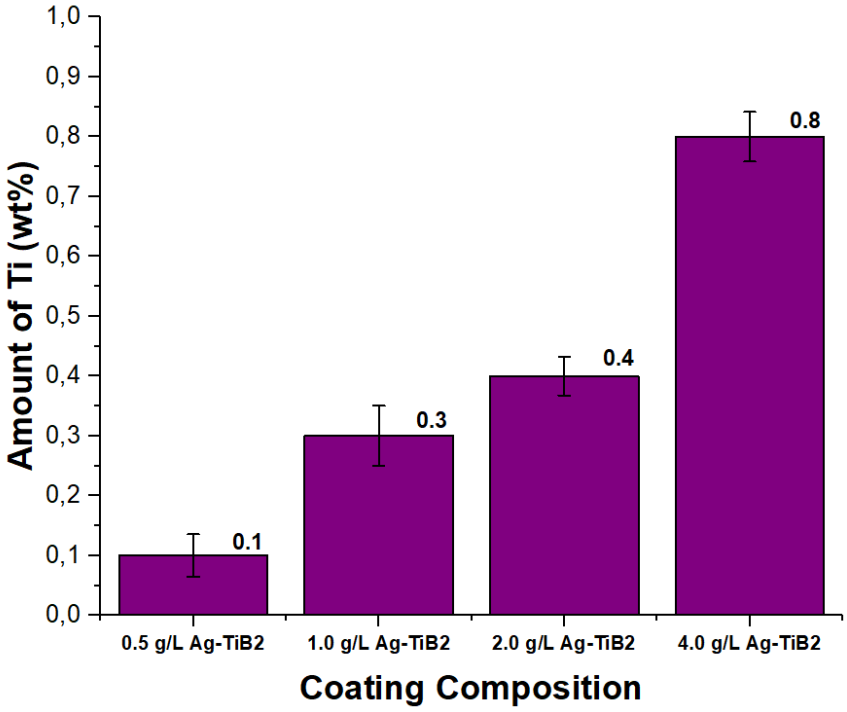

Figure 4.6 Weight percentages of Ti in 0.5, 1.0, 2.0 and 4.0 g/L Ag-TiB_2 nanocomposite coatings produced with DC method.

Comparison of Ti wt% for 1.0 g/L Ag-TiB_2 nanocomposite coatings produced via DC, PC and PRC electrodeposition methods is given in Figure 4.7. It can be clearly observed that the presence of TiB_2 effected by different current types. Ti ratio is the highest in PRC method coating (0.8 wt %) and lowest in DC coating (0.3 wt %) according to Figure 4.7. This can be resulted from the pulses during PRC method electrodeposition which caused higher incorporation of nano TiB_2 into Ag matrix. Similarly, T. Borkar et al. [78] investigated that the PC and PRC methods provide more amount of reinforcement for Ni matrix composite coatings. Also, Al-Falahi et al. [43] has found similar results with using PRC method for Ag-Gr nanocomposite coatings. They produced Ag-Gr nanocomposite coatings and obtained higher incorporation of nano Gr into Ag matrix is possible with the PRC method electrodeposition.

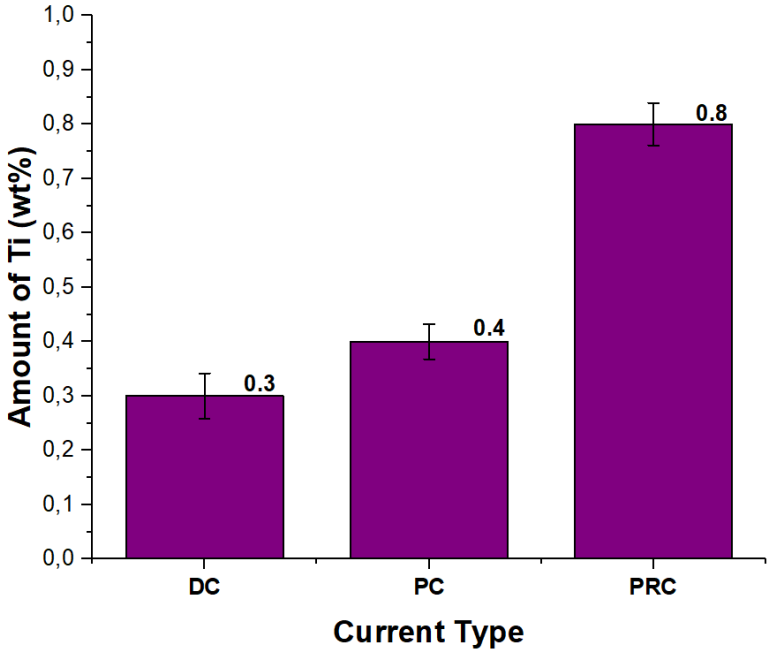

Figure 4.7 Weight percentages of Ti in 1.0 g/L Ag-TiB_2 nanocomposite coatings produced with DC, PC and PRC methods.

Also, EDS dot map analyze of 1.0 g/L Ag-TiB_2 nanocomposite coating produced with DC method is given in Figure 4.8. It can be observed that the elements (Ag, Ti and B) are homogeneously distributed on coatings. And according to Figure 4.9 which belongs to 4.0 g/L Ag-TiB_2 nanocomposite coating produced with DC method, it is clearly seen that the Ti and B elements are not homogeneously distributed as much as 1.0 g/L Ag-TiB_2 nanocomposite coating produced with DC method.

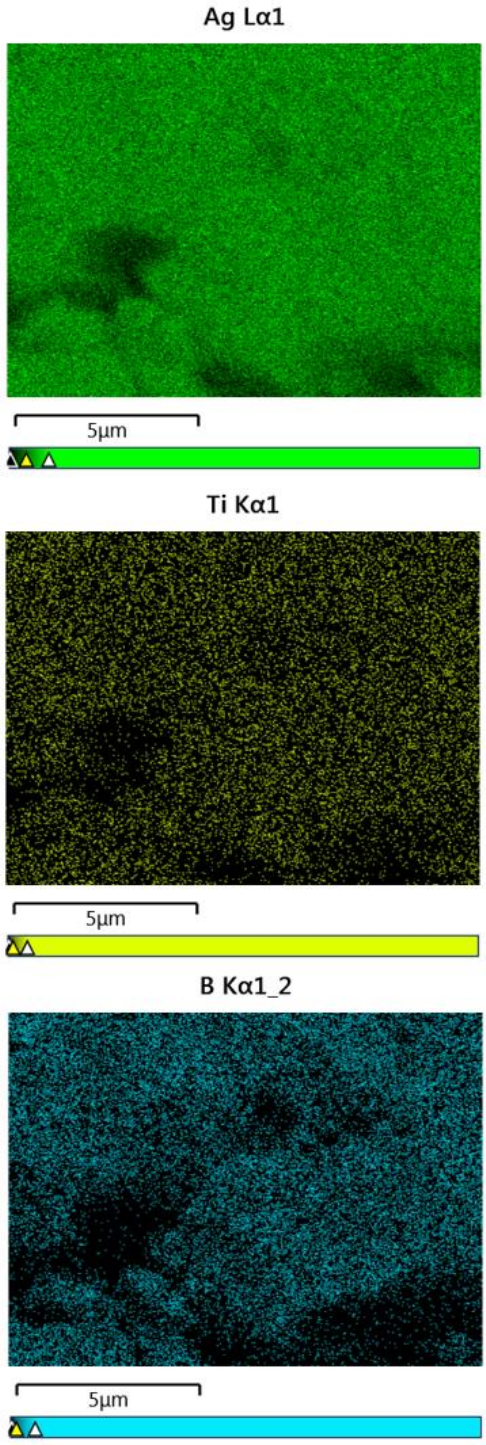

Figure 4. 8 EDS dot map analysis of 1.0 g/L Ag-TiB_2 nanocomposite coating produced via DC method.

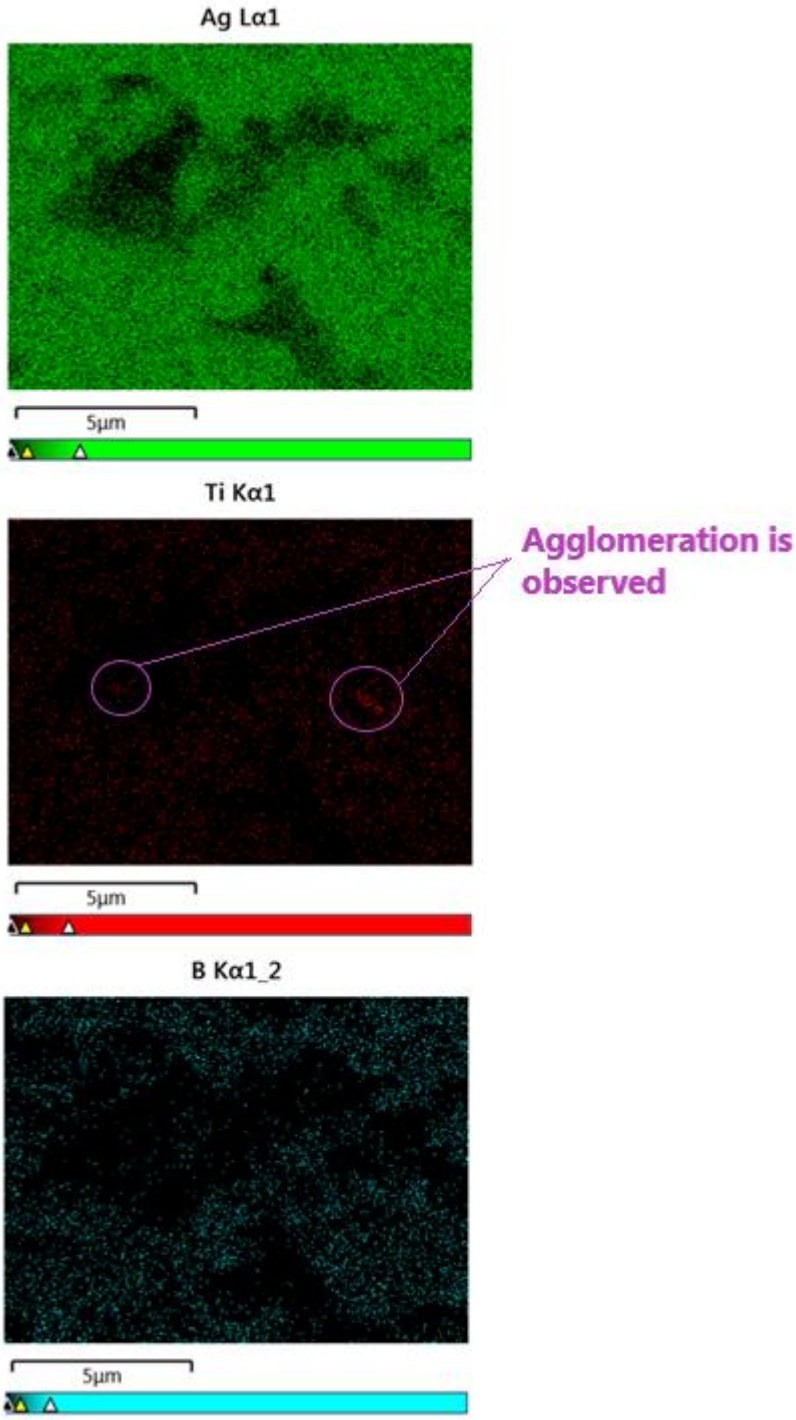

Figure 4. 9 EDS dot map analysis of 4.0 g/L Ag-TiB_2 nanocomposite coating produced via DC method.

4.1.3. X-Ray Diffraction (XRD) Analysis

The XRD analysis were used to get information about the crystallographic structures of unreinforced Ag and Ag-TiB_2 nanocomposite coatings deposited on copper cylindrical backings. Wavelength of X-Ray beam was chosen as 1.54059 Å. And XRD graphs were analyzed with 04-0783 JPCDS card number [83]. The XRD graphs of unreinforced Ag and 0.5, 1.0, 2.0 and 4.0 g/L Ag-TiB_2 nanocomposite coatings are presented in Figure 4.10.

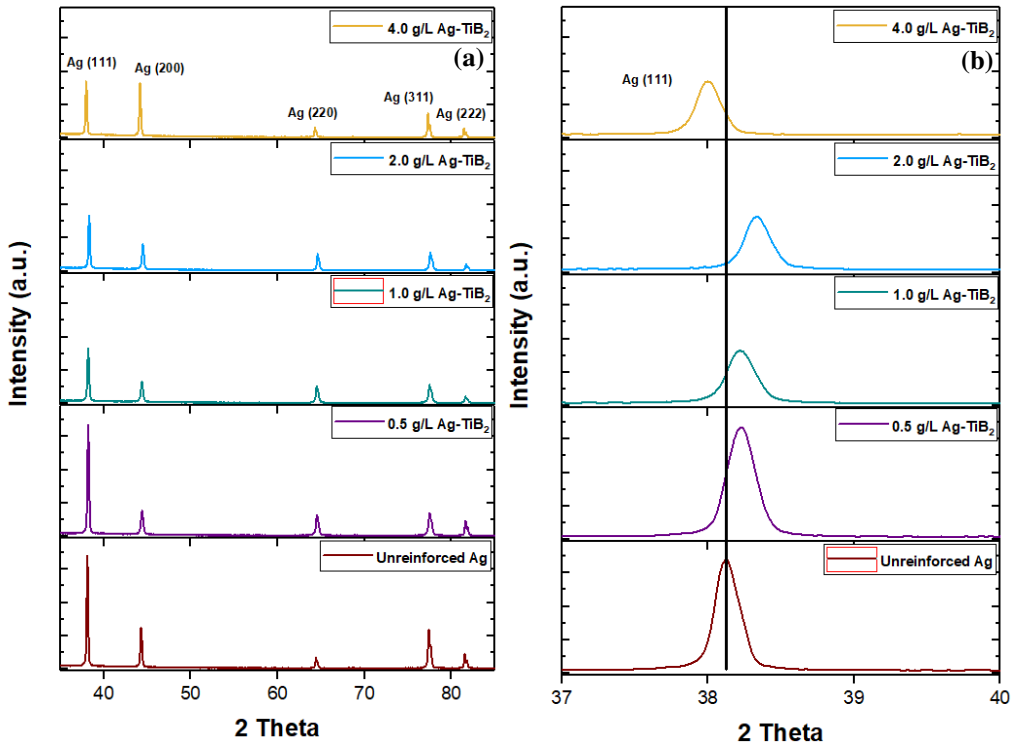

Figure 4.10 (a) Full spectrum and (b) Ag(111) peak of XRD results of unreinforced Ag and 0.5, 1.0, 2.0 and 4.0 g/L Ag- TiB_2 nanocomposite coatings produced by DC method.

Main peaks which are obtained from the Figure 4.10 are at 2θ=38.12˚, 2θ=44.3˚, 2θ=64.42˚, 2θ=77.4˚ which belongs to Unreinforced Ag, at 2θ=38.22˚, 2θ=44.44˚, 2θ=64.54˚, 2θ=77.48˚ for 0.5 g/L Ag-TiB_2 nanocomposite coating, at 2θ=38.22˚, 2θ=44.44˚, 2θ=64.54˚, 2θ=77.48˚ for 1.0 g/L Ag-TiB_2 nanocomposite coating, at 2θ=38.34˚, 2θ=44.5˚, 2θ=64.62˚, 2θ=77.58˚ for 2.0 g/L Ag-TiB_2 nanocomposite coating and at 2θ=38˚, 2θ=44.18˚, 2θ=64.32˚, 2θ=77.32˚ for 4.0 g/L Ag-TiB_2 nanocomposite coating. All the indicating peaks are corresponding to (111), (200),

(220) and (311) which are presented on XRD results as given in Figure 4.10(a). The highest peak intensity for each sample belongs to (111) reflection, therefore, preferred growth is this reflection. And, there is no reflection of TiB_2 among these five coatings due to small amount of reinforcement. However, it can be stated that the peak intensities are changed due to nano TiB_2 reinforcement into Ag matrix. While almost no significant change occurs on intensities of (220), (311) and (222) peaks, the intensities of (111) and (200) peaks significantly changed with the increased amount of nano TiB_2 reinforcement. The highest and lowest peak intensities of (111) reflection were observed from unreinforced Ag and 4.0 g/L Ag-TiB_2 nanocomposite coatings, respectively. The reason of decreasing (111) peak intensity with the higher amount of reinforcement is that the TiB_2 nanoparticles acts as a physical barrier and nanoparticles may provide new nucleation places caused refinement of Ag matrix. Similarly, Shi et al. [84] obtained that by the addition of CNTs, more nucleation sites resulted with smaller crystallite size was obtained for Ni-Co-CNTs composite coatings. Thus, in this study, more reinforcement (verified with EDS results) caused more less peak intensity of (111) reflection due to grain refinement of matrix. Also, it can be stated that a sufficient increase of (200) peak intensity with decrease of (111) peak intensity is observed with 4.0 g/L Ag-TiB_2 nanocomposite coating. This can be attributed to shifting preferred growth from (111) to (200) plane.

The (111) peak is presented in Figure 4.10(b). The decreasing intensity of (111) peak with the increased nano TiB_2 reinforcement can be clearly seen in the light of this figure. And, nano TiB_2 reinforcement into Ag matrix is resulted with the lattice distortion during coating and shifted the peaks. The peaks shifted to the right with 0.5, 1.0 and 2.0 g/L TiB_2 addition into electrolyte due to grain refinement effect of reinforcement on matrix material [74]. And (111) peak is shifted to the left with 4.0 g/L Ag-TiB_2 nanocomposite coating. This may be attributed to the higher reinforcement above a certain level resulted with agglomeration (also proven by the EDS map analyze on Figure 4.9). Agglomeration of second phase and obtaining less stress inside of the lattice structure caused (111) peak shifting to the left differently from the others.

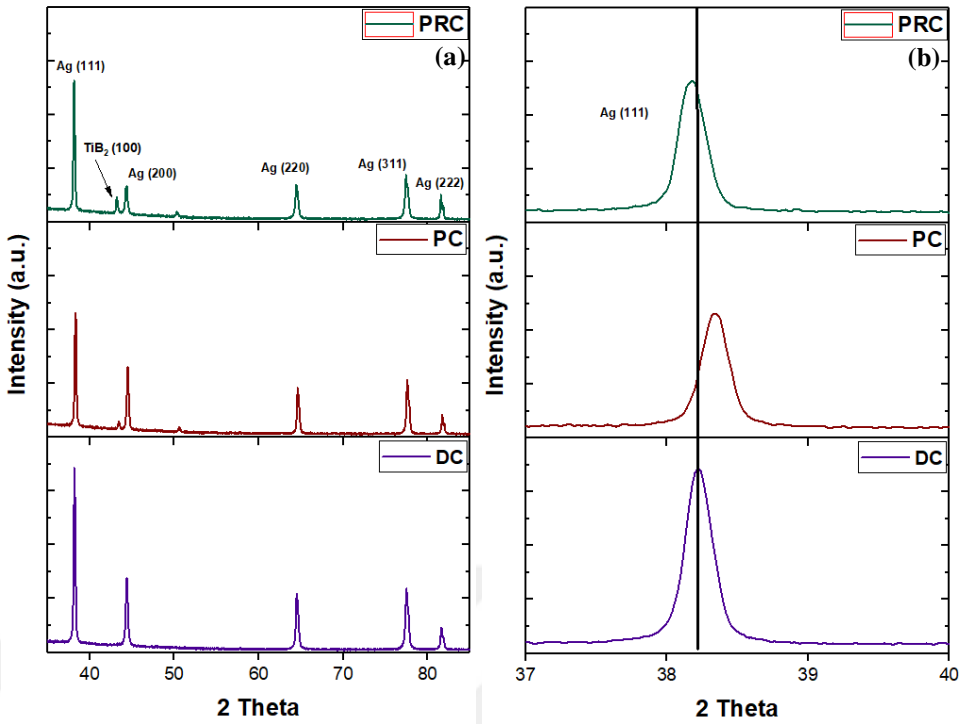

Figure 4.11 (a) Full spectrum and (b) Ag(111) peak of XRD results of 1.0 g/L Ag- TiB_2 nanocomposite coatings produced by DC, PC and PRC methods.

The XRD graphs of 1.0 g/L Ag-TiB_2 nanocomposite coatings produced via DC, PC and PRC methods are presented in Figure 4.11. Main peaks observed at 2θ=38.22˚, 2θ=44.44˚, 2θ=64.54˚, 2θ=77.48˚ which belongs to 1.0 g/L Ag-TiB_2 produced via DC method, at 2θ=38.34˚, 2θ=44.52˚, 2θ=64.64˚, 2θ=77.58˚ which belongs to 1.0 g/L Ag-TiB_2 produced via PC method and at 2θ=38.18˚, 2θ=44.38˚, 2θ=64.48˚, 2θ=77.44˚ which belongs to 1.0 g/L Ag-TiB_2 produced via PRC method. All the indicating peaks are corresponding to (111), (200), (220) and (311) of Ag which are presented on XRD results as given in Figure 4.10(a). Also, a Bragg reflection (100) of TiB_2 was observed in PC and PRC method coatings due to more reinforcement (also proved with the EDS results). This peak is observed at 2θ=43.46˚ for Ag-TiB_2 produced via PC method and at 2θ=43.22˚ for Ag-TiB_2 produced via PRC method. And the intensity of (100) of TiB_2 is increased with PRC method due to more reinforcement compared to PC method.

And, the highest peak intensity belongs to (111) reflection. Almost no significant change in (220), (311), and (222) peak intensities were observed. But, (111) and (200)

peak intensities were significantly changed due to applied current type. The peak intensity of (111) reflection was decreased with PC and PRC methods compared to DC method. The decreasing in peak intensity is a result of resisting grain growth of reinforcement. Since the reinforcement acts as a physical barrier, refining of Ag matrix resulted with smaller grains. Hence, it can be stated that PC and PRC methods provided smaller grains due to providing more nano TiB_2 reinforcement into Ag matrix and therefore, more grain refining compared to DC method. E. Gurcan et al. [56] obtained similar results with PC and PRC methods. They produced Ag-SiC nanocomposite coatings with using DC, PC and PRC methods. PC and PRC methods provided more nano SiC reinforcement into Ag matrix resulted with grain refining of matrix material. Similar results were also obtained by L.M. Chang et al. [85] that is about the effect of current type on composite coatings. They observed that the PRC method caused coatings with finer grains due to increased nucleation rate and nucleation centers. Another similar result was obtained by C. Shanthi et al. [77] that is PC method provides less porosity with fine grains compared to DC method. They studied for Ag coating produced by DC and PC methods and obtained finer grains with PC method because of the current efficiency is higher with this method. And at the same time, significant decrease on (200) peak intensity is observed with PRC method. Same wt% of Ti element were observed for 4.0 g/L Ag-TiB_2 nanocomposite coating produced with DC method and 1.0 g/L Ag-TiB_2 nanocomposite coating produced with PRC method. However, while compact and flat coating surface was observed with 1.0 g/L Ag-TiB_2 nanocomposite coating produced with PRC method, more rough and uneven coating surface was observed with 4.0 g/L Ag-TiB_2 nanocomposite coating produced with DC method. Therefore, decreased intensity of (200) peak can be an explanation of having more compact and flat coating surface compared to 4.0 g/L Ag-TiB_2 nanocomposite coating produced with DC method.

According to Figure 4.11(b) the (111) peak is shifted to the right in PC method coating. The peak shifts to the right can be a result of grain refinement [74]. Same peak is shifted to the left in PRC method coating due to having less stress on lattice.

4.2. Hardness Measurements of Coatings

Vickers microhardness test method was used to obtain hardness measurements on cross-sections of all coatings. The microhardness measurements of unreinforced Ag and Ag-TiB_2 nanocomposite coatings produced by DC method are presented in the Figure 4.12. It can be observed from the figure that nano TiB_2 reinforcement into the Ag matrix changed microhardness as expected. While the hardness of unreinforced Ag was 74.1 HV, 0.5 g/L nano TiB_2 addition into electrolyte caused increase in hardness and resulted with 80.7 HV. Thus, nano TiB_2 reinforcement into Ag matrix caused increase in hardness because of nanoparticles acting as physical barrier which inhibits grain growth of Ag matrix and resulted with smaller grains. Similarly, T. Borkar et al. [78] investigated that microhardness of Ni-AL_2O_3 composite coatings enhanced with the increased nanoparticle amount added into electrolyte because of the better dispersion strengthening effect.

Microhardness value is increased with the 1.0 g/L nano TiB_2 addition into electrolyte. But, with the 2.0 g/L addition of TiB_2, hardness started to decrease and measured as 79.5 HV for the 4.0 g/L Ag-TiB_2 nanocomposite coating. The grain refining effect due to acting as a physical barrier of nano TiB_2 on Ag matrix caused increase in hardness up to 1.0 g/L addition. However, increased agglomeration and roughness caused increased pores on coatings, thereby, hardness decreased with the addition of more than 1.0 g/L nano TiB_2 into electrolyte. Thus, highest hardness measurement was obtained from the 1.0 g/L Ag-TiB_2 nanocomposite coating (82.2 HV) among these five coatings.

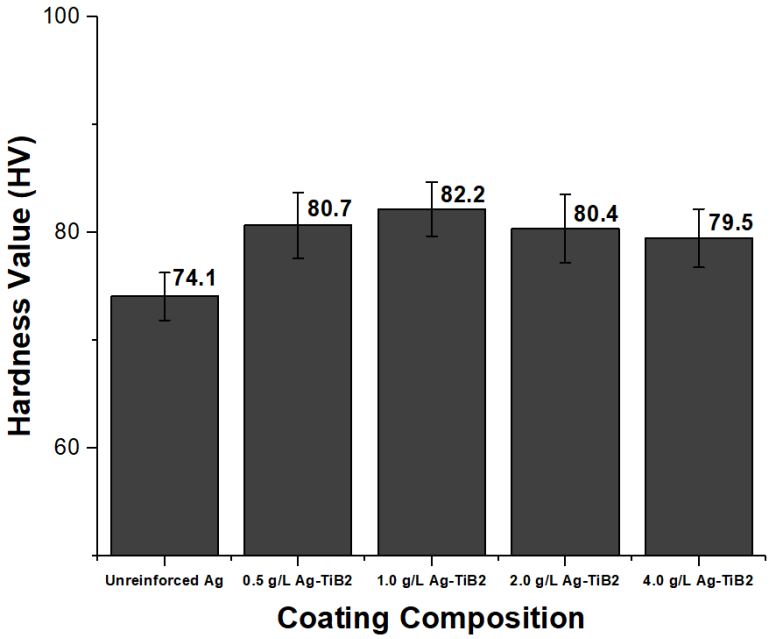

Figure 4.12 The microhardness measurements of unreinforced Ag and nanocomposite coatings.

Another comparison of hardness measurements is done on 1.0 g/L Ag-TiB_2 nanocomposite coatings which are deposited with different methods (DC, PC and PRC) as given in Figure 4.13. According to these results, since PC and PRC methods caused decreasing in grain size due to increased nucleation rate and centers, hardness values are increased with these methods compared to DC method. While DC method provided 82.2 HV hardness, PC and PRC method provided 82.8 and 85.3 HV hardness, respectively. Hence, the highest microhardness measurement was obtained as 85.3 HV of 1.0 g/L Ag-TiB_2 nanocomposite coating produced with PRC method due to its more grain refining effect than the other two methods. These results are agree with the EDS and XRD results. Karslioglu et al. [74] experienced that the PRC method provided superior microhardness on coatings compared to DC and PC methods. They investigated that introducing MWCNTs into Ni-Co matrix and using different methods (PC and PRC) improved hardness of coatings. Highest microhardness measurement was taken from composite coating produced with PRC method in the study.

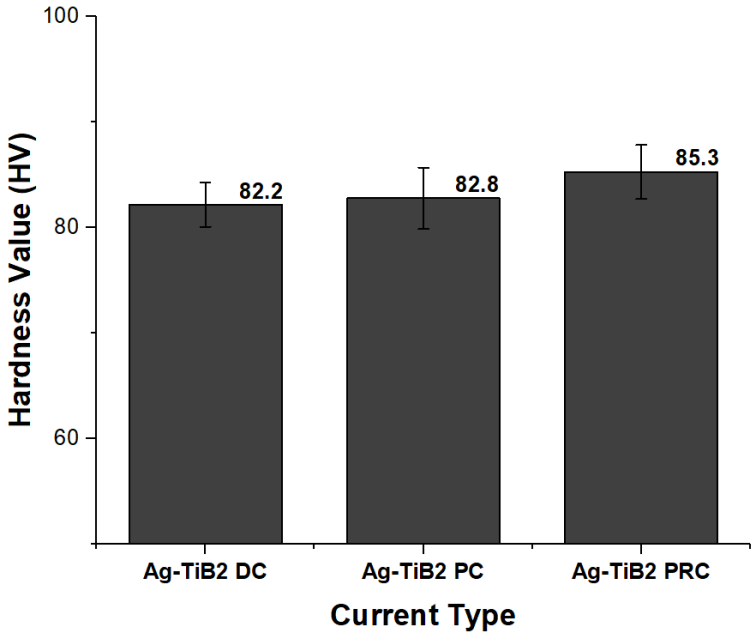

Figure 4.13 Effect of current type on hardness of nanocomposite coatings.

4.3. Deposition Rate of Coatings

The thicknesses of unreinforced Ag and Ag-TiB_2 nanocomposite coatings on cylindrical samples were obtained by cross-sectional analysis with using SEM. Figure 4.14 shows cross-sectional SEM image of unreinforced Ag coating. And the deposition rates of coatings were investigated from the divide of coating thicknesses by deposition process time (thickness (μm) / 120 min.). It was observed that the thickness of coatings differs due to amount of nano TiB_2 reinforcement into Ag matrix and current type used.

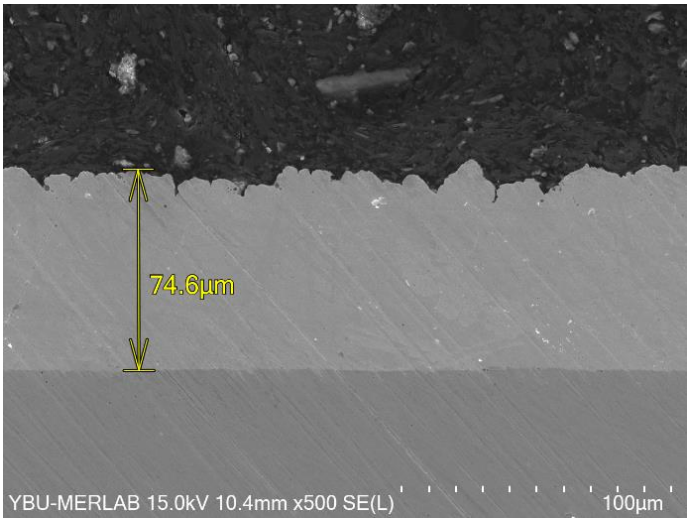

Figure 4.14 Cross-sectional SEM image of Ag deposited cylindrical sample.

A comparison of deposition rates of unreinforced Ag and 0.5, 1.0, 2.0 and 4.0 g/L Ag-TiB_2 nanocomposite coatings is presented in Figure 4.15. Nano TiB_2 reinforcement into Ag matrix caused increasing thicknesses, thereby, increasing deposition rates. More nano TiB_2 reinforcement into matrix resulted with higher thicknesses, therefore, higher deposition rates. Thickness layer measurements were 67.2, 73.0, 75.25, 77.3 and 87.45 µm for unreinforced Ag and 0.5, 1.0, 2.0 and 4.0 g/L Ag-TiB_2 nanocomposite coatings, respectively. Georgiza et al. [86] achieved similar results with the Ni-B-SiC composite coatings by electroless deposition on metal substrates. They observed that coating thickness increases with the incorporation of SiC particles into coatings compared to non-composite coating.

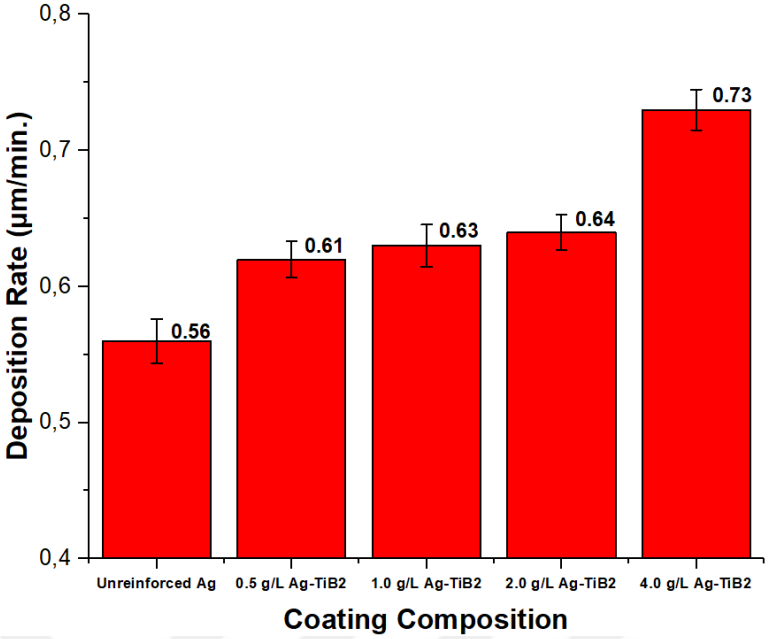

Figure 4.15 Deposition rate of unreinforced Ag and Ag-TiB_2 nanocomposite coatings produced with DC method electrodeposition.

Same comparison was obtained for 1.0 g/L Ag-TiB_2 nanocomposite coatings produced with DC, PC and PRC method electrodeposition. Figure 4.16 presents the deposition rates of these three coatings. And the deposition rate is increased with PC and PRC methods. According to EDS results, more nano TiB_2 reinforcement was obtained with PC and PRC methods compared to DC method electrodeposition. Thus, obtaining higher thicknesses, therefore higher deposition rates with PC and PRC methods is not a surprise. Because of providing more reinforcement property of PRC method during this study, the highest deposition rate among these three coatings was observed in 1.0 g/L Ag-TiB_2 nanocomposite coating which deposited with PRC method electrodeposition (Figure 4.16). Also, thickness layer measurements were 75.25, 81.45 and 88.6 µm for 1.0 g/L Ag-TiB_2 nanocomposite coatings produced with DC, PC and PRC methods, respectively.

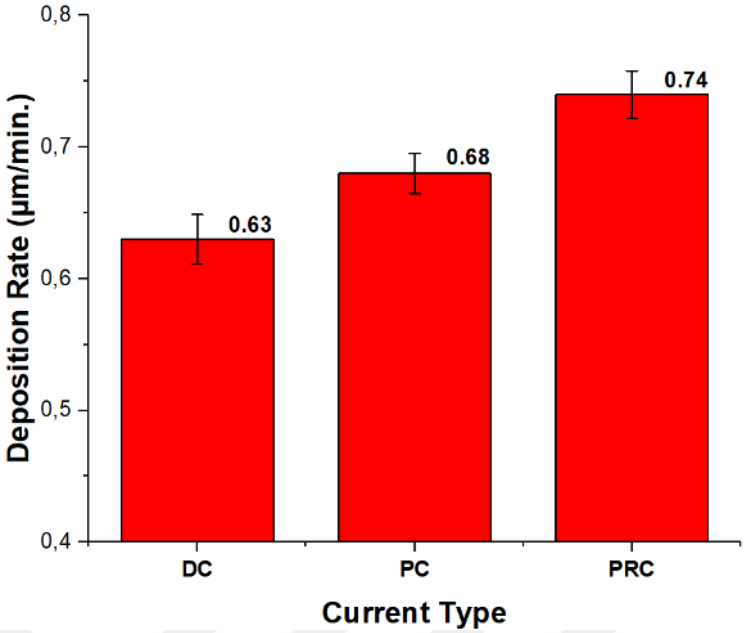

Figure 4.16 Deposition rates of 1.0 g/L Ag-TiB_2 nanocomposite coatings produced with DC, PC and PRC method electrodeposition.

4.4. Electrical Resistivity Measurements

Electrical resistivity measurements with using two-point test method were done on coatings which are deposited on copper cylindrical backings. Electrical resistivity measurements of the unreinforced Ag and Ag-TiB_2 nanocomposite coatings deposited on copper cylindrical samples are given in Figure 4.17. According to the results, TiB_2 reinforcement was caused a small increase in electrical resistivity when unreinforced Ag and 0.5 g/L Ag-TiB_2 nanocomposite coatings are compared. The electrical resistivity was increased as the amount of nano TiB_2 reinforcement into Ag matrix is increased (in the light of EDS results). And the highest electrical resistivity measurement is 0.294 ohm which belongs to 4.0 g/L Ag-TiB_2 nanocomposite coating. It is clearly stated in the literature that smaller grains cause obtaining more grain boundaries resulted with increased electrical resistivity. Because, since the grain boundaries are irregular regions, they affect the electrical conduction in a negative way [43,87]. And it was observed that nano TiB_2 reinforcement caused grain refining of Ag matrix because reinforcement's acting as a physical barrier. 4.0 g/L nano TiB_2 addition caused highest grain refining and highest reinforcement amount among these

five coatings according to XRD and EDS results. Hence, more grain boundaries caused highest electrical resistivity which is measured with the 4.0 g/L Ag-TiB_2 nanocomposite coating. Thus, these results are harmonized with the EDS and XRD results.

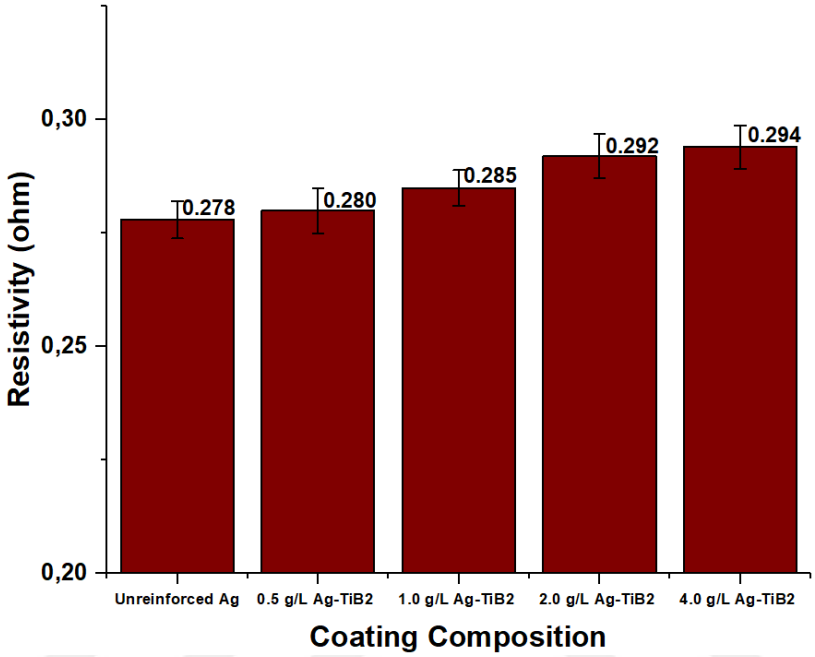

Figure 4.17 Electrical resistivity measurements of unreinforced Ag and 0.5, 1.0, 2.0 and 4.0 g/L Ag-TiB_2 nanocomposite coatings.

Electrical resistivity measurements were carried out for 1.0 g/L Ag-TiB_2 nanocomposite coatings which are produced with using different electrodeposition methods DC, PC and PRC (Figure 4.18). Due to smaller grains with more grain boundaries in PC and PRC method coatings, increase in electrical resistivity was expected. With accordance of XRD and EDS results, the least electrical resistivity measurement was 0.285 ohm which belongs to 1.0 g/L Ag-TiB_2 nanocomposite coating deposited with DC method. However, changing current type caused increased reinforcement amount, smaller grains of matrix material and increase in grain boundaries. Hence, electrical resistivity of PC and PRC is higher than DC method coating. The highest electrical resistivity was measured as 0.297 ohm which belongs to 1.0 g/L Ag-TiB_2 nanocomposite coating produced via PRC method.

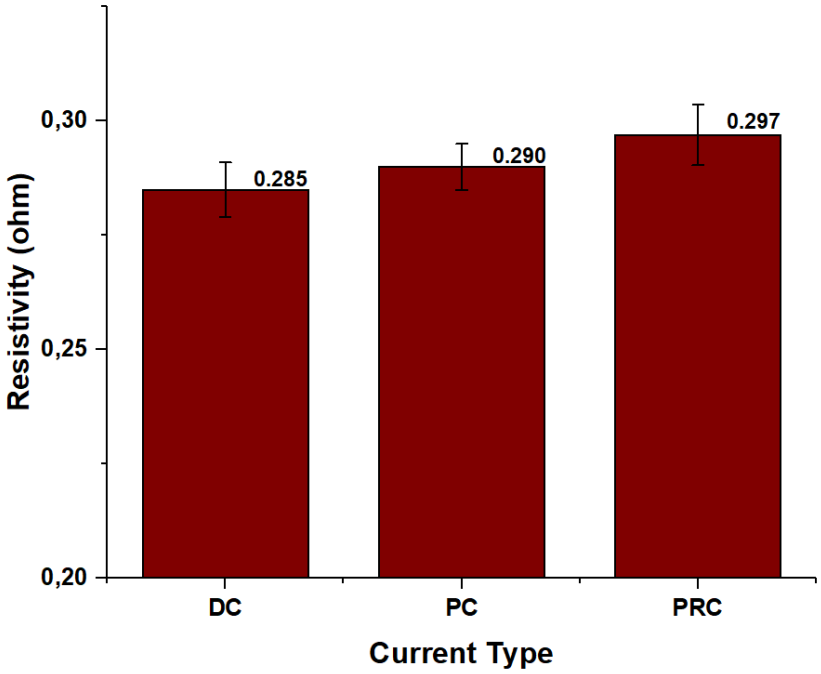

Figure 4.189 Electrical resistivity measurements of 1.0 g/L Ag-TiB_2 nanocomposite coatings produced with different current types DC, PC and PRC.

4.5. Electrical Contact Test

Electrical contact buttons which are deposited with the unreinforced Ag and Ag-TiB_2 nanocomposite coatings were subjected to electrical contact tests. A handmade electrical contact test device is used to obtain contact tests. During these tests, the temperature of contact buttons were recorded in order to get information about contact resistance of buttons. The reason to record temperature during contact test for obtaining contact resistance is the knowledge of resistance increases with increased temperature [43]. And, as can be seen from the Figure 4.19 and Figure 4.20, temperature increase of contact buttons during contact tests differ from each other due to amount of nano TiB_2 reinforcement.

Firstly, electrical contact tests were applied on copper backings of buttons which were not deposited. These contact buttons are break down after 1139 number of contact cycles as presented in Figure 4.19. Therefore, it can be stated that with the unreinforced Ag and nanocomposite coatings, contacts with longer service life are obtained. And the temperature increase of unreinforced Ag during 10000 cycles of contact test is the

least one compared to other four nanocomposite coatings according to Figure 4.19. It can be noted that nano TiB_2 reinforcement into Ag matrix caused faster temperature increase compared to unreinforced Ag coating. After 10000 cycle of contact test, the temperatures of unreinforced Ag and 0.5, 1.0, 2.0 and 4.0 g/L Ag-TiB_2 nanocomposite coatings were measured as 43.85, 44.53, 46.06, 49.75 and 57.00°C, respectively. Therefore, contact resistance is increased with the increased nano TiB_2 reinforcement into Ag matrix.

Also, as number of contact cycle increases, oxide films are formed and caused increasing contact resistance [43]. And it must be stated that 4.0 g/L Ag-TiB_2 nanocomposite coating resulted with highest temperature increase and contact resistance compared to other four coatings (Figure 4.19). Hence, increased nano TiB_2 reinforcement into Ag matrix and oxide films which occur due to increased number of contact cycles caused increasing contact resistance.

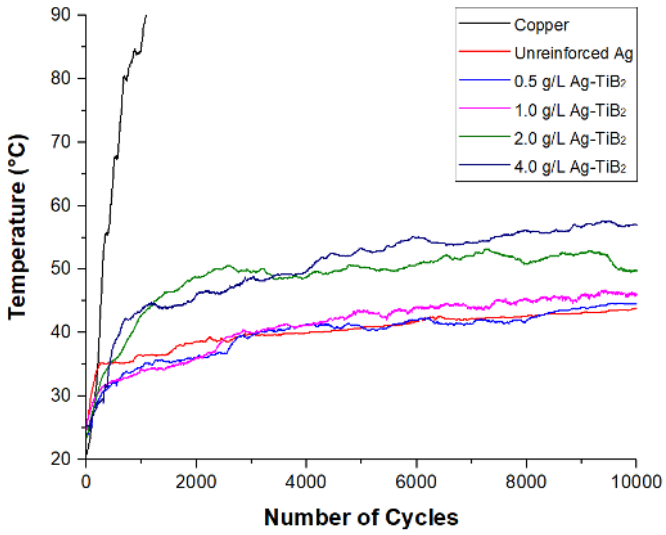

Figure 4.19 Electrical performance measurements of unreinforced Ag and 0.5, 1.0, 2.0 and 4.0 g/L Ag-TiB_2 nanocomposite coatings produced with DC method.

And 3000 cycle of contact test were done on 1.0 g/L Ag-TiB_2 nanocomposite coatings produced via PC and PRC methods. Therefore, another comparison of contact resistance measures up to 3000 cycle is done as shown in Figure 4.20. The highest temperature increase, thereby, highest contact resistance was observed in PRC method coating. It can be stated that more nano TiB_2 reinforcement caused higher contact

resistivity. Also, increased number of contact cycles causes increased contact resistivity due to oxide films formed because of the arc between contact pairs [43]. Hence, the PRC method coating was given highest contact resistance compared to DC and PC. Also, forward contact tests were applied on 1.0 g/L Ag-TiB_2 nanocomposite coatings produced by DC method. These contact buttons are brake down after 44706 contact cycles.

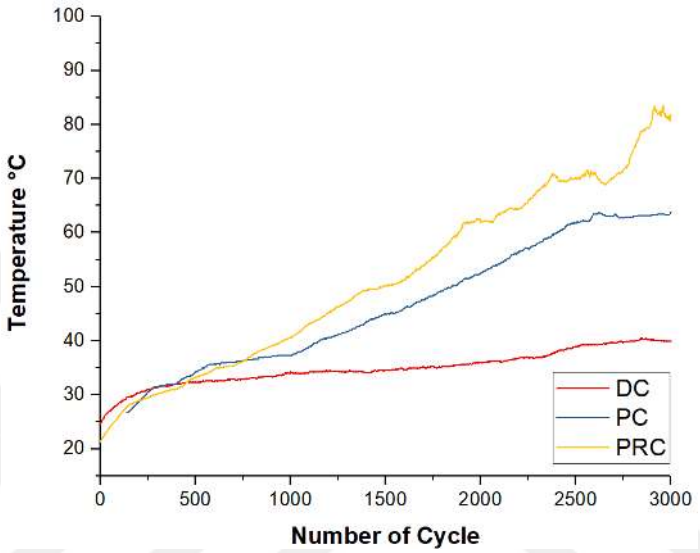

Figure 4.20 Electrical performance measurements of 1.0 g/L Ag-TiB_2 nanocomposite coatings produced with DC, PC and PRC methods.

4.6. Effect of Contact Test on Coating Surface Morphology

The contact tests were applied to unreinforced Ag and Ag-TiB_2 nanocomposite coatings which are deposited on copper backings of contact buttons. Each contact pairs (one up-contact button and two down-contact buttons) were placed into contact unit of HDC6 contactor of Himel brand which is placed in a handmade contact test device. While electrical contact test was taking place, up contact button moved downward until contact take place with down contact button. The contact tests were taken place at a constant load of 4 kW with a ~18 A /DC current and voltage of 220 V. And after contact tests, SEM analyzes were done on coatings to observe the effect of contact test on coating morphology. Thus, characterization of arc erosion morphology of contact buttons which are deposited with the unreinforced Ag and 0.5, 1.0, 2.0 and 4.0 g/L Ag-TiB_2 nanocomposite coatings is presented in Figure 4.21.

It is clearly observed from the Figure 4.21, addition of nano TiB_2 into electrolyte is significantly changed surface morphologies after 10000 cycle of contact test. With the 0.5 g/L addition of nano TiB_2 into electrolyte, surface morphology has changed significantly compared to unreinforced Ag. More homogeneous deformation was observed in 0.5 g/L Ag-TiB_2 nanocomposite coating compared to unreinforced Ag coating. This can be attributed to the increased hardness with the 0.5 g/L Ag-TiB_2 nanocomposite coating despite of increased electrical resistivity. And, with the 1.0 g/L addition of nano TiB_2 into electrolyte, the surface becomes more flat and less erosion pits were observed due to increased hardness.

Electrical resistivity was always increased with the increased nano TiB_2 reinforcement into Ag matrix, and hardness was first increased with the increased nano TiB_2 reinforcement. However, with the 2.0 and 4.0 g/L Ag-TiB_2 nanocomposite coatings, hardness was decreased due to agglomeration and porosities. Therefore, more uneven contact surface with rougher erosion pits after contact tests was observed with the 2.0 and 4.0 g/L Ag-TiB_2 nanocomposite coatings. Hence, the most preferable erosion behavior among these five coatings is observed for contact buttons which are deposited with the 1.0 g/L Ag-TiB_2 nanocomposite coating produced via DC method.

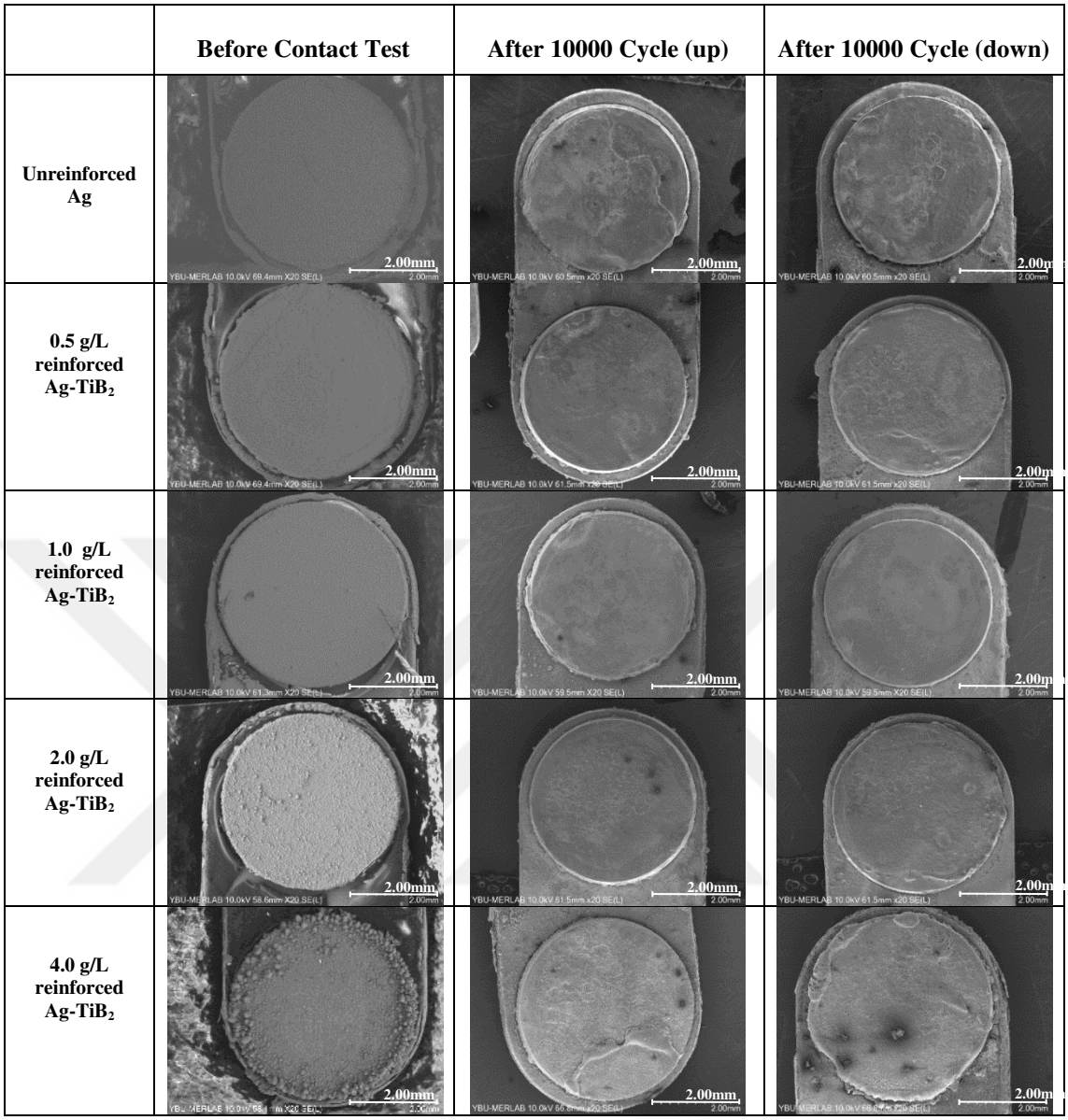

Figure 4.21 Effect of nano TiB_2 reinforcement amount on Ag-TiB_2 nanocomposites electrical contact performance.

Surface morphologies of 1.0 g/L Ag-TiB_2 nanocomposite coatings produced via PC and PRC methods are represented in Figure 4.22. Changing current methods has a significant effect on surface morphologies of contact surfaces after 3000 cycle of contact test. It can be clearly stated that PC and PRC method electrodeposition did not provide preferable erosion behavior after contact tests. PC and PRC methods caused higher erosion pits and more melting deformation compared to DC method (Figure 4.21) because of their higher electrical resistivity. Therefore, the highest melting and

evaporation of material was observed with the PRC method due to higher arc erosion behavior.

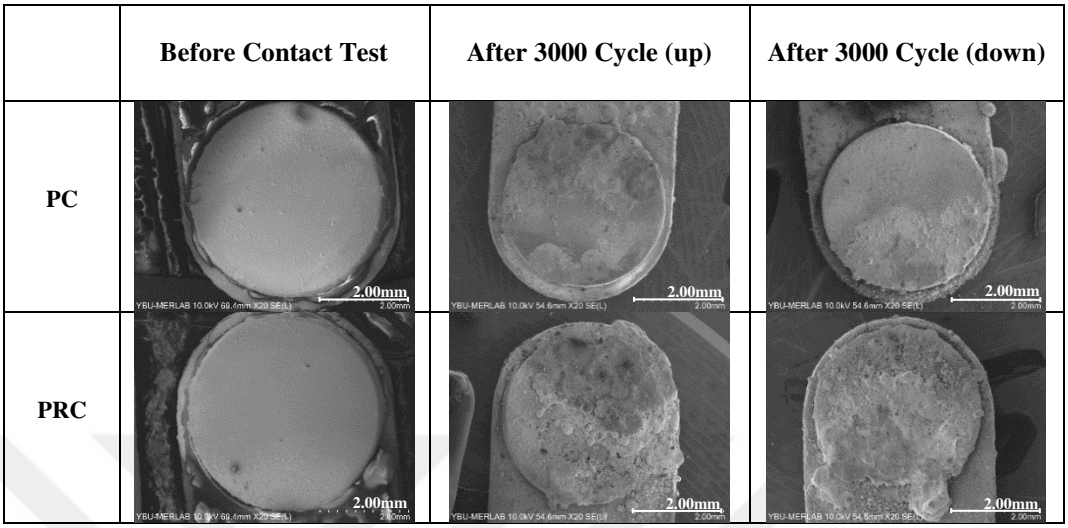

Figure 4.22 Effect of current type on 1.0 g/L Ag-TiB_2 nanocomposites produced by DC, PC and PRC methods electrical contact performance.

Higher contact resistance caused increase in contact surface temperature and resulted with melting on contact surface most for PRC method coating. As melting occurs, a molten bridge occurs between contact pairs and this situation causes arc generation and erosion. Hence, due to highest contact resistance caused by PRC method on coatings, the most uneven surface morphology was observed with this method after 3000 cycle of contact test. Similarly, E. Gurcan et al. [56] was studied with the Ag-SiC nanocomposite coatings produced by electrodeposition method. They observed that DC method caused better surface morphology after contact test compared to PC and PRC methods.

And, the preferable erosion behavior with more even surface among all coatings was observed in 1.0 g/L Ag-TiB_2 nanocomposite coating produced via DC method electrodeposition due to lower contact resistance and highest hardness (Figure 4.21). Therefore, the contact tests were done on 1.0 g/L Ag-TiB_2 nanocomposite coatings produced with DC method until its break-down. The surface morphology of this coating after 10000 and 30000 cycle of contact tests is presented in Figure 4.23. According to SEM images, contact surface (after 10000 contact cycle) consists some

erosion pits. And after 30000 contact cycle, surface become more uneven with rougher erosion pits due to increased temperature during contact test. And with the 44706 contact cycles, temperature of contact buttons reached 90°C and contacts were break-down. Hence, surface morphology of these contact pairs after contact tests shows that 1.0 g/L Ag-TiB_2 nanocomposite coatings produced via DC method provide preferable arc erosion behavior.

Before Contact Test	After 10000 cycle of contact test	After 30000 cycle of contact test
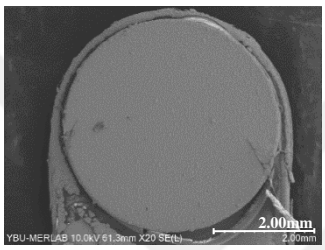	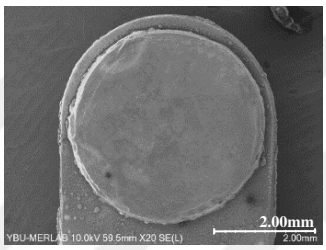	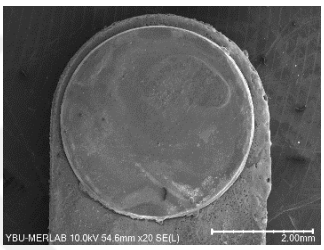

Figure 4.23 SEM images of 1.0 g/L Ag-TiB_2 nanocomposite coating produced by DC method before test, after 10000 and 30000 electrical contact performance tests.

4.7. Corrosion Resistance Properties

Corrosion resistance tests were obtained due to investigate the effect of nano TiB_2 reinforcement on corrosion properties of Ag. A comparison to obtain effect of different amount of nano TiB_2 reinforcement on corrosion resistance is presented in Figure 4.24. It can be clearly observed that different amounts of nano TiB_2 reinforcement into Ag matrix changed corrosion resistance. 0.5 g/L Ag-TiB_2 nanocomposite coating have a little more positive potential compared to unreinforced Ag coating. And this increase in corrosion resistance starts to significantly increase with more nano TiB_2 reinforcement into matrix material. With the 1.0, 2.0 and 4.0 g/L Ag-TiB_2 nanocomposite coatings more positive potential, therefore, higher corrosion resistance was obtained. Also, it must be stated that the corrosion rate measurements were done on these coatings and the results are $8.923x10^{-005}$, $3.361x10^{-005}$, $1.619x10^{-003}$, $2.659x10^{-003}$ and $8.045x10^{-003}$ gram/hour for unreinforced Ag and 0.5, 1.0, 2.0 and 4.0 g/L Ag-TiB_2 nanocomposite coatings, respectively. J. Li et al. [88] investigated similar

results. They observed that the corrosion resistance of nanocomposite coatings (Ni-Titania nanocomposite) is increased with the increased reinforcement into matrix.

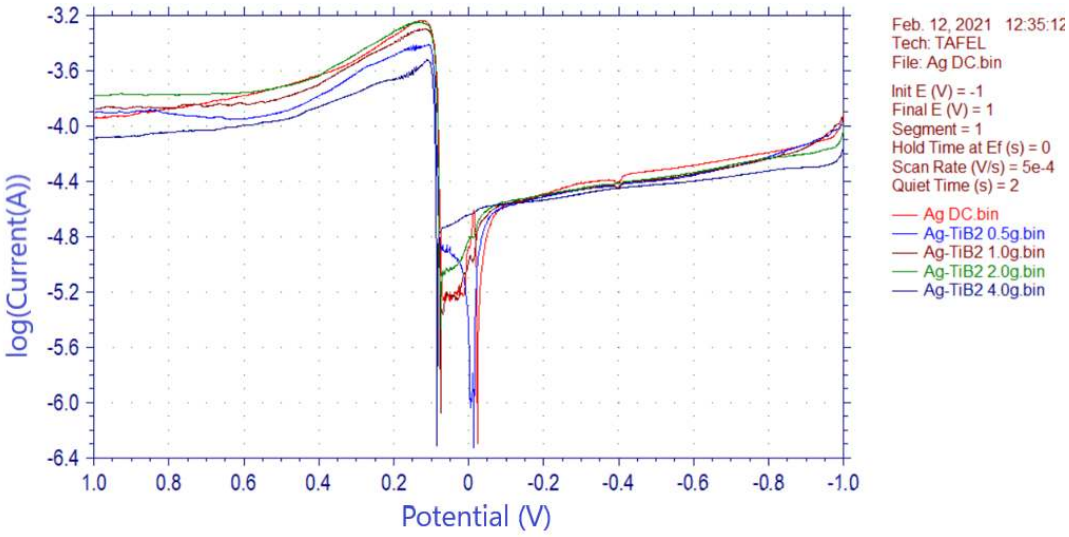

Figure 4.24 Potendiodynamic polarization curves of Ag-TiB_2 nanocomposite coatings produced with different amount of nano TiB_2.

Another comparison of corrosion resistance is investigated for 1.0 g/L Ag-TiB_2 nanocomposite coatings produced via DC, PC and PRC methods. Polarization curve of this comparison is presented in Figure 4.25. As it can be assumed from the figure that the current type significantly changed the corrosion potential of 1.0 g/L Ag-TiB_2 nanocomposite coatings. Corrosion potential becomes more negative from DC to PRC method. Hence, it can be stated that PC and PRC methods caused decreasing of corrosion resistance compared to DC method. This can be attributed to the increased surface area which resulted from grain refining comes with the PC and PRC methods. Decreased grain size with PC and PRC methods caused more surface area of matrix material. Thereby, removing of particles from the coating surface becomes easier. Also, smaller grains with PC and PRC methods causes increasing grain boundaries. Grain boundaries have low stability and high energies, thereby, they are easily corrode [89]. Consequently, 1.0 g/L Ag-TiB_2 nanocomposite coating produced via DC method showed best corrosion resistance among these three coatings due to bigger grains and less grain boundaries. Also, corrosion rates are $1.619x10^{-003}$, $1.765x10^{-004}$ and $1.113x10^{-004}$ gram/hour for 1.0 g/L Ag-TiB_2 nanocomposite coatings produced via DC, PC and PRC methods, respectively.

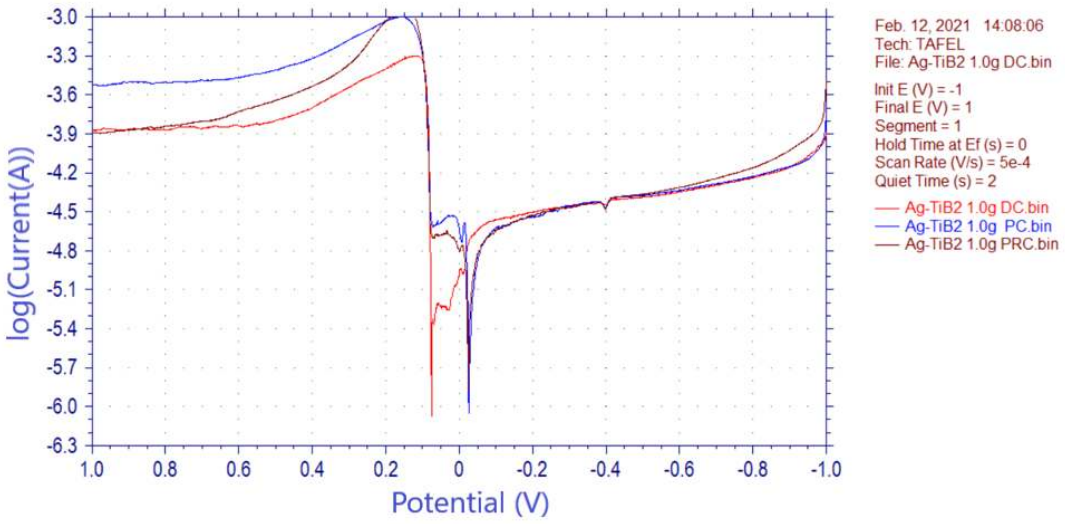

Figure 4.25 Potendiodynamic polarization curves of 1.0 g/L Ag- TiB_2 nanocomposite coatings produced with DC, PC, PRC methods.

CHAPTER 5

Conclusion and Future Work

5.1. Conclusion

In this study, unreinforced Ag and Ag-TiB_2 nanocomposite coatings with different amount of reinforcements were produced on cylindrical copper substrates and copper backings on electrical contact buttons. The effects of nano TiB_2 reinforcement and different amounts of nano TiB_2 added into electrolyte were examined. Also, DC, PC and PRC methods used to produce 1.0 g/L Ag-TiB_2 nanocomposite coatings by electrodeposition method in order to obtain the effects of current types. Influence of these parameters on coatings was investigated with the characterization methods such as Scanning Electron Microscope (SEM), Energy Dispersive Spectroscopy (EDS), X-ray Diffraction Analysis (XRD), Vickers Microhardness Test, deposition rate measurements by Cross-Sectional Analysis, Electrical Resistivity Measurements, Electrical Contact Performance Test and Corrosion Resistance Tests. And the results can be summarized as:

1. In the light of SEM analysis, introducing nano TiB_2 into Ag matrix caused more flat and compact coating surface with small particles. With 0.5 and 1.0 g/L nano TiB_2 addition into electrolyte, more compact and flatter surface is observed compared to unreinforced Ag coating. Incorporation of nano TiB_2 into matrix decreased roughness. However, with 2.0 and 4.0 g/L nano TiB_2 addition into electrolyte, rougher surface with coarser particles are observed. This is attributed to agglomeration of nano TiB_2 with above a certain level of amount. Most homogeneous and compact surface is observed with 1.0 g/L Ag- TiB_2 nanocomposite coating produced with DC method among these five coatings.

   And another comparison was done for 1.0 g/L Ag-TiB_2 nanocomposites deposited via DC, PC and PRC method electrodeposition. Homogeneous and flat coating surface was obtained with DC method. However, bigger

particles were observed with the PC and PRC methods. But still, homogeneous and flat coating surface is observed with PC and PRC methods.

2. EDS results showed that as the amount of nano TiB_2 added into electrolyte increases, Ti wt% increases too. And the highest Ti ratio in coatings was observed with 4.0 g/L Ag-TiB_2 nanocomposite coatings compared to 0.5, 1.0 and 2.0 g/L Ag-TiB_2 nanocomposite coatings. Therefore, it can be stated that higher concentration of nano TiB_2 into electrolyte enhanced adsorption rate.

   With the PC and PRC methods, more nano TiB_2 reinforcement into Ag matrix was provided. The highest Ti ratio among DC, PC and PRC method coatings was observed with PRC method deposited nanocomposite coating due to pulses in PRC which cause higher incorporation. Also, agglomeration is proven with the EDS map analysis of 4.0 g/L Ag-TiB_2 nanocomposite coating.

3. Bragg reflections (111), (200), (220), (311), and (222) of Ag were obtained from XRD results for all coatings. Preferred orientation was (111) reflection and its intensity was changed due to amount of reinforcement and used current type. Firstly, it was observed that with the increased amount of nano TiB_2 reinforcement, the intensity of (111) peak was decreased due to smaller grains.

   This can be attributed to the reinforcement acting as a physical barrier and providing new nucleation places resulted with the grain refining of matrix. Hence, smallest grains with smallest intensity of (111) peak was belong to 4.0 g/L Ag-TiB_2 nanocomposite coating among unreinforced Ag and 0.5, 1.0, 2.0 and 4.0 g/L Ag-TiB_2 nanocomposite coatings.

   And peak shifting was observed due to lattice distortion resulted from reinforcement. Peaks shifted to the right with 0.5, 1.0 and 2.0 g/L nano TiB_2 addition due to smaller grains. And same peak is shifted to the left with 4.0 g/L nano TiB_2 addition into electrolyte due to obtaining less stress in lattice. XRD analysis of coatings produced with using different current types (PC and PRC) showed all Ag peaks and also a peak of TiB_2. This is also a proof

of more TiB_2 reinforcement into Ag matrix is possible with these two methods. The intensity of TiB_2 (100) peak increases with the PRC method compared to PC method. This is also an indicator of having more reinforcement with PRC method. Also, the lowest intensity of (111) reflection was observed with PRC method coating due to smaller grains compared to DC and PC methods. In addition, the (111) reflection shifted to right with PC method due to smaller grains and shifted to left with PRC method due to obtaining agglomeration and less stress on lattice.

4. According to hardness measurements, nano TiB_2 reinforcement into Ag matrix effected hardness of coatings. Among coatings which are deposited with different amounts of reinforcement by using DC method, 1.0 g/L Ag-TiB_2 nanocomposite coating was ensured highest hardness measurement due to smaller grains. Having smaller grains was continued with the 2.0 and 4.0 g/L addition of nano TiB_2 (according to XRD results), however, hardness is decreased with these two compositions due to obtained agglomeration and porosities.

   And since PC and PRC methods ensured more reinforcement into Ag matrix and caused more grain refining than DC method, hardness of coatings was increased with these two methods. In PRC method, highest hardness measurement was obtained because of providing more TiB_2 reinforcement, grain refining and more nucleation centers of Ag matrix.

5. Deposition rates of all coatings were obtained by dividing coating thicknesses with deposition time (thickness (μm) / 120 min.). With the increased amount of reinforcement into Ag matrix, deposition rate always increased and 0.73 μm/min. deposition rate (highest among coatings which are deposited with different amounts of reinforcement by using DC method) was measured for 4.0 g/L Ag-TiB_2 nanocomposite coating.

   Due to applied current type during electrodeposition, amount of reinforcement into Ag matrix was changed according to EDS results. And the deposition rates of 1.0 g/L Ag-TiB_2 nanocomposite coatings produced with DC, PC and PRC is changed due to nano TiB_2 reinforcement into Ag matrix. 0.63 μm/min. deposition rate was measured for DC method and this

number is increased with the PC and PRC methods due to increased amount of reinforcement. Highest deposition rate was 0.74 μm/min. obtained with PRC method coating.

6. Two-point test was applied on unreinforced Ag and nanocomposite coatings deposited on copper cylindrical samples to obtain electrical resistivity of coatings. And according to results, nano TiB_2 reinforcement caused increasing electrical resistivity. This can be attributed to having smaller grains with more grain boundaries. Since grain boundaries prevent motion of electrons, electrical resistivity increases with more grain boundaries (smaller grains). Therefore, highest electrical resistivity was obtained with 4.0 g/L Ag-TiB_2 nanocomposite coating compared to unreinforced Ag and 0.5, 1.0 and 2.0 g/L Ag-TiB_2 nanocomposite coatings. And different current methods were changed the electrical resistivity of coatings. PRC method caused highest electrical resistivity compared to DC and PC methods. This can be attributed to increased grain boundaries which prevent motion of electrons in PRC method. Hence, highest electrical resistivity of 0.297 ohm is measured with PRC method.
7. Electrical contact tests were applied on all coatings deposited on contact buttons. Firstly, unreinforced Ag coating showed least temperature increase up to 10000 contact cycle compared to 0.5, 1.0, 2.0 and 4.0 g/L Ag-TiB_2 nanocomposite coatings. Nano TiB_2 reinforcement caused higher temperature increase during 10000 contact cycle. Hence, it can be stated that nano TiB_2 reinforcement caused higher contact resistance. And with the increased amount of reinforcement, contact resistance is increased too. Also contact tests were applied on copper which already exists on contact buttons (sample which were not deposited). These contact buttons break down after 1139 contact cycle. Hence, providing longer service life with unreinforced Ag and 0.5, 1.0, 2.0 and 4.0 g/L Ag-TiB_2 nanocomposite coatings was proven.

   And 3000 contact cycle was applied on 1.0 g/L Ag-TiB_2 nanocomposite coatings produced with PC and PRC methods. PC and PRC methods caused

higher temperature increase compared to DC method. And, highest contact resistance is observed with PRC method with highest temperature increase.

8. And to obtain arc erosion morphologies after contact tests, SEM images were analyzed for unreinforced Ag and 0.5, 1.0, 2.0 and 4.0 g/L Ag-TiB_2 nanocomposite coatings. With the increased reinforcement up to 1.0 g/L Ag-TiB_2 nanocomposite coatings, coatings provide preferable morphology. But with the 2.0 and 4.0 g/L Ag-TiB_2 nanocomposite coatings, surface morphology of coatings become more uneven with rougher erosion pits. The most preferable surface morphology after contact test was observed with 1.0 g/L Ag-TiB_2 nanocomposite coating due to its highest hardness value among these five coatings. But with the increased reinforcement amount in coating, unwanted surface morphology after contact was observed because of the increased electrical resistivity and decreased hardness.

   And 3000 contact cycle was applied on 1.0 g/L Ag-TiB_2 nanocomposite coatings produced via PC and PRC methods. And due to increased electrical resistivity, PC and PRC methods did not provide preferable erosion behavior compared to DC coating. Hence, 1.0 g/L Ag-TiB_2 nanocomposite coating produced by DC method showed best contact performance due to its preferable electrical resistivity and highest hardness value. Therefore, electrical contact tests was applied on these coatings until their break-down. And they break-down after 44706 cycle of contact test.
9. Corrosion resistance studies were applied on coatings which are produced on copper cylindrical backings. And it was observed that nano TiB_2 reinforcement caused higher corrosion resistance of coatings compared to unreinforced Ag coating. And the highest corrosion resistance was observed with the 4.0 g/L Ag-TiB_2 nanocomposite coating.

   And with different current types (PC and PRC), corrosion resistance of coatings was decreased. The reinforcement amount into matrix was increased with PC and PRC methods, however, the grain refining of matrix resulted with increased surface area of matrix material. Therefore,

removing of particles from surface become easier. Hence, DC method showed higher corrosion resistance than PC and PRC methods.

Consequently, nano TiB_2 reinforcement into Ag matrix caused smaller grains with more compact coating surface, increased electrical resistivity, increased deposition rate, increased contact resistance and increased hardness. Among all coatings, 1.0 g/L Ag-TiB_2 (produced by DC method) nanocomposite coating showed best contact erosion behavior after contact test. This can be attributed to its highest hardness measure, having most compact and flat coating surface, having preferable electrical resistivity and contact resistance compared to other coatings. Hence, contact tests were applied on these buttons and they break down after 44706 contact cycle.

5.2. Future Works

- Effect of using different current densities, duty cycles during electrodeposition process can be examined.
- Electrical contact tests must be done on all of nanocomposite coatings until break-down of contacts.
- For all coatings, surface morphologies can be examined by 3D profiler before and after contact tests.

REFERENCES

1. Findik, F., Uzun, H. Microstructure, hardness and electrical properties of silver-based refractory contact materials. Mater. Des., (*24*), 489-492. 2003

2. Wu, C., Yi, D., Weng, W., Li, S., Zhou, J., Zheng, F. Arc erosion behavior of Ag/Ni electrical contact materials. Mater. Des., (*85*), 511-519. 2015

3. Zhou, Y.X., Xue, Y.L., Zhou, K. Failure analysis of arc ablated tungsten-copper electrical contacts. Vacuum, (*164*), 390–395. 2019

4. Biyik, S., Aydin, M. Investigation of the Effect of Different Current Loads on the Arc-Erosion Performance of Electrical Contacts. Acta Phys. Pol. A, (*129*), 656-660. 2016

5. Zhang, X., Zhang, Y., Tian, B., Jia, Y., Liu, Y., Song, K., Volinsky, A. A. Thermal deformation behavior of the Al2O3-Cu/(W, Cr) electrical contacts. Vacuum, (*164*), 361–366. 2019
6. Kiliç, A. Gelişmiş Ülkelerde Ve Türkiye'de Yangin Nedenleri. Yangın ve Güvenlik Dergisi, (*200*), 8-10. 2018
7. Hou, M., Li, L., Zhuang, M. Research on application mechanism of cadmium in new energy vehicle charging group. IOP Conf. Ser.: Earth Environ. Sci., (*227*). 2019

8. Lungu, M., Gavriliu, S., Nitu, S., Canta, T., Sin, D., Budrugeac, P., Patroi, D. New Ag-SnO2-MeO ecological advanced materials for electrical contacts used in electromagnetic contactors. J. Optoelectron. Adv. Mater., (*10*), 1064 – 1068. 2008

9. Imrell, T. The importance of the thickness of silver coating in the corrosion behavior of copper contacts. ABB Corporate Research, S-721 78 Vasteras Sweden.
10. Karslioglu, R., Al-Falahi, L. Electrical contact performance of various electro-deposited graphene reinforced silver-based nanocomposites. Mater. Test., (*62*), (4), 401-407. 2020

11. Perottoni, C.A., Pereira, A.S., da Jornada, J.A.H. Periodic Hartree–Fock linear combination of crystalline orbitals calculation of the structure, equation of state and elastic properties of titanium diboride. J. Phys.: Condens. Matter, (*12*), 7205–7222. 2000
12. YIH, P., CHUNG, D. D. L. Titanium diboride copper-matrix composites. J. Mater. Sci., (*32*), 1703-1709. 1997
13. Nguyen-Tri, P., Nguyen, T. A., Carriere, P., Xuan, C. N. Review Article Nanocomposite Coatings: Preparation, Characterization, Properties, and Applications. Int. J. Corros., (*2018*). 2018
14. Varvani-Farahani, A. Composite Materials: Characterization, Fabrication and Application-Research Challenges and Directions. Appl. Compos Mater, (*17*), 63–67. 2009
15. Kesarwani, P., Jahan, S., Kesarwani, K. Composites: Classification and its manufacturing Process. Int. j. appl. res., (*1*), (9), 352-358. 2015
16. Wang, J.F., Liew, K.M. On the study of elastic properties of CNT-reinforced composites based on element-free MLS method with nanoscale cylindrical representative volume element. Compos. Struct., (124), 1–9. 2015
17. Kaya, A. İ. Kompozit Malzemeler ve Özellikleri. Putech & Composites, 38-45. 2016
18. Patil, P.R., Kadam, G.A. Overview on Comparative Study of Characterization of Properties of Natural Fiber Composites. International Research Journal of Engineering and Technology, (*4*), (7). 2017
19. Haghshenas, M. Metal–Matrix Composites. Comprehensive Composite Materials, (*6*), 57-66. 2000
20. Yao, J., Zhou, Z., Zhou, H. Introduction to Composite Materials. *Highway Engineering Composite Material and Its Application*. (1st edition) pp. (3-6). Singapore: Springer. 2019
21. Kalemtaş, A. Seramik Matrisli Kompozit Malzemeler. Putech & Composites, 20-26. 2015
22. Rajak, D. K., Pagar, D. D., Kumar, R., Pruncu, C. I. Recent progress of reinforcement materials: a comprehensive overview of composite materials. J. Mater. Res. Technol., (*8*), (6), 6354–6374. 2019

23. Kessler, M. R. Polymer Matrix Composites: A Perspective for a Special Issue of Polymer Reviews. Polym. Rev., (*52*), (3), 229-233. 2012

24. Miracle, D.B. Metal matrix composites – From science to technological significance. Compos. Sci. Technol., (*65*), 2526–2540. 2005

25. Roylance, D. Introduction to Composite Materials. Retrieved May 28, 2021, https://resources.saylor.org/wwwresources/archived/site/wp-content/uploads/2012/09/ME1022.2.3.pdf. March 24, 2000
26. Sharma, A. K., Bhandari, R., Aherwar, A., Rimašauskiene, R. Matrix materials used in composites: A comprehensive study. Mater. Today: Proc., (*21*), (3), 1559-1562. 2020
27. Blessley, D. Composite Materials. Retrieved May 28, 2021, https://www.academia.edu/7487930/Module_1_General_Introduction_M1_General_Introduction.
28. Composite Materials Reinforcement basics. Retrived May 27, 2021, http://metalurji.mu.edu.tr/Icerik/metalurji.mu.edu.tr/Sayfa/Composite%20Materials2(1).pdf.
29. U.S. Congress, Office of Technology Assessment. Advanced Materials by Design (Card number: 87-619860). Washington DC: U.S. Government Printing Office, 1988
30. Kedari, S. *Metal Matrix Composites (MMCs).* Retrieved May 28, 2021, https://www.slideshare.net/kedarisantosh/metal-matrix-composite?qid=13fa0ca6-c6f9-45fa-b02c-0dfae2fc2200&v=&b=&from_search=2. 2014
31. Braunovic, M., Konchits, V. V., Myshkin, N. K. *Electrical Contacts: Fundamentals, Applications and Technology* (1st edition). USA: CRC Press. 2007
32. Electrical Contacts. (n.d.). Retrieved from https://www.norstaninc.com/blog/electrical-contacts/
33. Kardys, G. *The ımportance of Electrical Contacts and Contact Resistance.* Retrived March 2, 2021, https://electronics360.globalspec.com/article/11182/the-importance-of-electrical-contactsandcontactresistance#:~:text=Electrical%20contacts%2C%20connectors%20and%20connections,possibility%20of%20loss%20of%20life. 2018

34. Chapman, D. Copper in Electrical Contacts. Copper Development Association Publication (223), 39 pages. Retrived March 5, 2021. 2015
35. Timsit, R.S. Electrical Contact Resistance: Properties of Stationary Interfaces. IEEE. 1998
36. Książkiewicz, A. Contact materials used in low voltage electrical relays. Comput. Appl. Eng., (*13*), 300-309. 2015
37. Song, J., Koch, C., Wang, L. Correlation between Wear Resistance and Lifetime of Electrical Contacts. Adv. Tribol. 2012
38. Sung, I.H., Kim, J.W., Noh, H.J., Jang, H. Effect of displacement and humidity on contact resistance of copper electrical contacts. Tribol. Int., (*95*), 256–261. 2015
39. Barceloux D.G., Barceloux, D. Copper. J. Toxicol. Clin. Toxicol., (*37*), (2), 217-230. 1999
40. *Global electrical contacts and contacts materials market report 2019*. Retrived March 3, 2021, https://www.marketintellica.com/report/MI24904-global-electrical-contacts-and-contacts-materials. 2019
41. Slade, P.G. (Ed.) *Electrical Contacts: Principles and Applications* (2nd edition). CRC Press, 2014.
42. *Contact Materials for Electrical Engineering*. Retrived March 5, 2021, https://www.electrical-contacts-wiki.com/index.php/Contact_Materials_for_Electrical_Engineering. 2014
43. Lujain, A. Graphene Reinforced Sılver Nanocomposite by Electrodeposition for Electrical Contact Materials. Thesis (M.Sc.), Yildirim Beyazit University. 2018
44. Malaki, M., Xu, W., Kasar, A. K., Menezes, P. L., Dieringa, H., Varma, R. S., Gupta, M. Advanced Metal Matrix Nanocomposites. Metals, (*9*), (330). 2019
45. Omanović-Mikličanin, E., Badnjević, A., Kazlagić, A., Hajlovac, M., Nanocomposites: a brief review. Health and Technol., (*10*), 51-59. 2020
46. Singh, V. B., Singh D. K. An Overview on the Preparation, Characterization and Properties of Electrodeposited-Metal Matrix Nanocomposites. Nanosci. Technol., (*1*), (3), 1-20. 2014.
47. Casati, R., Vedani, M. Metal Matrix Composites Reinforced by Nano-Particles. Metals, (*4*), 65-83. 2014

48. Huang, X., Feng, Y., Li, L., Li, Z. Erosion Behavior of a Cu-Ti_3AlC_2 Cathode by Multi-Electric Arc. Materials, (*12*), (18), 2019.
49. Cao, G., Zhang, Y., Liu, J., Nan, D., Liu, H. Contrastive Research on Electrical Contact Performance for Contact Materials of Cu-SnO_2 and Cu-ZnO_2 Alloys. Materials Research, (*22*), (3). 2019
50. Karslioglu, R. Effect of Bath Composition on Structural Properties of Graphene Reinforcement Silver Matrix produced by Electroless Deposition. International Journal of Engineering Research and Development, (*11*), (2), 637-642. 2019
51. MAO, F. *Synthesis, Characterization, and Evaluation of Ag-based Electrical Contact Materials*. Digital Comprehensive Summaries of Uppsala Dissertations from the Faculty of Science and Technology, 98 pages. 2017
52. Śleziona, J., Wieczorek, J., Dyzia, M. Mechanical properties of silver matrix composites reinforced with ceramic particles. J. Achiev. Mater. Manuf., (*17*), (1-2), 165-168. 2006
53. Huang, X., Feng, Y., Qian, G., Zhou, Z. Arc ablation properties of Ti_3SiC_2 material. Ceramics International, (45), 20297–20306. 2019
54. Ding, J., Tian, W., Wang, D., Zhang, P., Chen, J., Zhang, Y., Sun, Z. Corrosion and degradation mechanism of Ag/Ti_3AlC_2 composites under dynamic electric arc discharge. Corrosion Science, (156), 147–160. 2019
55. Ding, J., Tian, W., Wang, D., Zhang, P., Chen, J., Zhang, Y., Sun, Z. Microstructure evolution, oxidation behavior and corrosion mechanism of Ag/Ti2SnC composite during dynamic electric arc discharging. J. Alloys Compd., (*785*), 1086-1096. 2019
56. Gurcan, E. Silicon Carbide Reinforcement Silver Metal Matrix Nanocomposite Coatings on Copper by Different Electrodeposition Methods and Amount of Silicon Carbide. Thesis (M.Sc.), Yildirim Beyazit University. 2020
57. *Titanium Diboride.* Retrived March 12, 2021, https://en.wikipedia.org/wiki/Titanium_diboride. 2020
58. Fahrenholtz, W. G., Wuchina, E. J., Lee, W. E., Zhou, Y. (Ed.). *Ultra-High Temperature Ceramics: Materials for Extreme Environment Applications* (1st edition). Wiley. 2014

59. Rabiezadeh, A., Hadian, A. M., Ataie, A. Synthesis and sintering of TiB_2 nanoparticles. Ceramics International, (*40*), (10), 15775-15782. 2014
60. Sanchez, C.M.T., Plata, B. R., Maia da Costa, M.E.H., Freire Jr., F.L. Titanium diboride thin films produced by dc-magnetron sputtering: Structural and mechanical properties. Surf. Coat. Tech., (*205*), 3698–3702. 2011
61. Munro, R. G. Material Properties of Titanium Diboride. J. Res. Natl. Inst. Stand. Technol., (105), 709-720. 2000
62. Vinokurov, A. A., Kovalev, D. Y., Korobov, I. I., Kravchenko, O. V., Konovalikhin, S. V., Khomenko, N. Y., Kalinnikov, G.V., Nadkhina, S. E., Shilkin, S. P. Synthesis, Structure, and Properties of Titanium Diboride Nanoparticles. Inorg. Mater., (*56*), (11), 1127-1132. 2020
63. Shayesteh, F., Delbari, S.A., Ahmadi, Z., Shokouhimehr, M., Asl, M.S. Influence of TiN dopant on microstructure of TiB_2 ceramic sintered by spark plasma. Ceramics International, (*45*), 5306–5311. 2019
64. Konstantinov, A.S., Bazhin, P.M., Stolin, A.M., Kostitsyna, E.V., Ignatov, A.S. Ti--B--Based Composite Materials: Properties, Basic Fabrication Methods, and Fields of Application. Compos. - A: Appl. Sci. Manuf., (*108*), 79-88. 2018
65. Cotton, J, *Titanium Diboride (TiB_2) - Properties and Applications.* Retrived March 10, 2021, https://www.azom.com/article.aspx?ArticleID=492. 2001
66. Kumar, A.M., Rathanasamy, R., Kaliyannan, G.V., Chinnasamy, M., Palaniappan, S.K. Fabrication Methods of Organic/Inorganic Nanocomposite Coatings. *Polymer Coatings: Technology and Applications.* (1st edition) pp. (21-40). USA: Scrivener Publishing LLC. 2020
67. Purohit, B., Kumar, A., Mahato, K., Chandra, P. Electrodeposition of Metallic Nanostructures for Biosensing Applications in Health Care. J. Sci. Res., (*64*), (1), 68-73. 2020
68. Al-Bat'hi S.A.M. Electrodeposition of Nanostructure Materials. *Electroplating of Nanostructures*. (1st edition) pp. (4-11). Croatia, InTech. 2015
69. Low, C.T.J., Wills, R.G.A., Walsh, F.C. Electrodeposition of composite coatings containing nanoparticles in a metal deposit. Surf. Coat. Tech., (*201*), 371–383. 2006

70. Saidin, N.U., Ying, K.K., Khuan, N.I. Electrodeposition: Principles, Applications and Methods. Industrial Technology Division, Malaysian Nuclear Agency, Kajang, Selangor.
71. Mangalaraj, D., Poongodi, S. Electrodeposition—A Simple and Effective Method for the Preparation of Metal Oxide Nanostructured Thin Films. *Recent Trends in Materials Science and Applications.* (1st edition) pp. (51-52). Switzerland, Springer International Publishing. 2017
72. Jayakkrıshnan, D.S. Electrodeposition: the versatile technique for nanomaterials. *Corrosion Protection and Control Using Nanomaterials.* (1st edition) pp. (86-93). USA, Woodhead Publishing. 2012
73. Li, R., Hou, Y., Dong, Q., Su, P., Ju, P., Liang, J. Wear and corrosion resistance of Co–P coatings: the effects of current modes. RSC Adv., (*8*), 895–903. 2018
74. Karslioglu, R., Akbulut, H. Comparison Microstructure and Sliding Wear Properties of Nickel-Cobalt/CNT Composite Coatings by DC, PC and PRC Current Electrodeposition. Appl. Surf. Sci., (*353*), 615-627. 2015
75. Chandrasekar, M.S., Pushpavanam, M. Pulse and pulse reverse plating—Conceptual, advantages and applications. Electrochimica Acta, (*53*), 3313–3322. 2008
76. Stappers, L., Ngoy, C.N., Zhang, W., Toben, M., Fransaer, J. Electrodeposition of Silver-Carbon Coatings with Low Contact Resistance and Wear Rate. J. Electrochem. Soc., (*160*), (4), D137-D145. 2013
77. Shanthi, C., Barathan, S., Jaiswal, R., Arunachalam, R.M. Study of surface morphology in DC and pulse plating of silver alloy. Indian Journal of Engineering & Materials Sciences, (*16*), 128-132. 2009
78. Borkar, T., Harimkar, S.P. Effect of electrodeposition conditions and reinforcement content on microstructure and tribological properties of nickel composite coatings. Surf. Coat. Tech., (*205*), 4124–4134. 2011
79. Li, H., Wang, X., Xi, Y., Zhu, T., Guo, X. Effect of Ni addition on the arc-erosion behavior of $AgTiB_2$ contact material. Vacuum, (*161*), 361–370. 2019
80. Xi, Y., Wang, X., Zhou, Z., Li, H., Guo, X. Material transfer behavior of $AgTiB_2$ contact under different contact forces and electrode gaps. Trans. Nonferrous Met. Soc. China, (*29*), 1046−1056. 2019

81. Xianhui, W., Hao, Y., Shuhua, L., Mabao, L., Qida, L. Effect of TiB_2 Particle Size on Erosion Behavior of Ag-4wt% TiB_2 Composite. Rare Metal Materials and Engineering, (*44*), (11), 2612-2617. 2015
82. Eslami, M., Golestani-fard, F., Saghafian, H., Robin, A. Study on tribological behavior of electrodeposited Cu–Si_3N_4 composite coatings. Mater. Des., (*58*), 557-569. 2014
83. Punjabi, K., Yedurkar, S., Doshi, S., Deshapnde, S., Vaidya, S. Biosynthesis of silver nanoparticles by Pseudomonas spp. isolated from effluent of an electroplating industry. IET Nanotechnology, (*11*), (5), 584-590. 2017
84. Shi, L., Sun, C.F., Gao, P., Zhou, F., Liu, W.M. Electrodeposition and characterization of Ni–Co–carbon nanotubes composite coatings. Surf. Coat. Tech., (*200*), 4870– 4875. 2006
85. Chang, L.M., An, M.Z., Shi, S.Y. Microstructure and characterization of Ni-Co/Al2O3 composite coatings by pulse reversal electrodeposit. Mater. Chem. Phys., (*100*), 395–399. 2006
86. Georgiza, E., Gouda, V., Vassiliou, P. Production and properties of composite electroless Ni-B-SiC coatings. Surf. Coat. Tech., (*325*), 46-51. 2017
87. Karslioglu, R., Uysal, M., Akbulut, H. The effect of substrate temperature on the electrical and optic properties of nanocrystalline tin oxide coatings produced by APCVD. J. Cryst. Growth, (*327*), (1), 22-26. 2011
88. Li, J., Sun, Y., Sun, X., Qiao, J. Mechanical and corrosion-resistance performance of electrodeposited titania–nickel nanocomposite coatings. Surf. Coat. Tech., (*192*), 331 – 335. 2005
89. Barut, U., Karslioglu, R. Influence of current type on tribological and corrosion properties of nickel boron coatings produced by electrodeposition. Kovove Materialy, (*57*), 167–175. 2019

APPENDICES

Appendix A: Program which is used for electrical contact tests.

Appendix A- Program which is used for electrical contact tests.

```
#include <OneWire.h>
#include <DallasTemperature.h>

#define but 4
#define out 5


unsigned int say=0,t=0;
#define ONE_WIRE_BUS_1 2
OneWire oneWire_in(ONE_WIRE_BUS_1);
DallasTemperature sensor_inhouse(&oneWire_in);
void setup() {
  // put your setup code here, to run once:
  pinMode(but, INPUT);
  pinMode(out, OUTPUT);
    Serial.begin(9600);
    sensor_inhouse.begin();
}

void loop() {
  // put your main code here, to run repeatedly:
  if(say<65000){
  digitalWrite(out,HIGH);
       delay(100);
    sensor_inhouse.requestTemperatures();
    Serial.print(say, DEC);
    Serial.print(";");
    Serial.println(sensor_inhouse.getTempCByIndex(0));
      delay(1000);
   digitalWrite(out,LOW);
         delay(2000);
      say++;
  }
}
```

CURRICULUM VITAE

PERSONAL INFORMATION

Name Surname **:** Dila COŞMUŞ

Date of Birth **:**

Phone :

E-mail **:**

EDUCATION

Bachelor **:** Ankara Yıldırım Beyazıt University, Metallurgical and Materials Engineering (2012-2018)

Master Degree **:** Ankara Yıldırım Beyazıt University, Materials Engineering (2019-2022)

Foreign Language

English